AD

MIPR 2.00518
AMCMS Code: 5910.21.63443
HDL Proj: E05E6

IN 124 L24

HDL-TR-1602

TERMINAL RESPONSE OF BRAIDED-SHIELD CABLES TO EXTERNAL MONOCHROMATIC ELECTROMAGNETIC FIELDS

by

Sidney Frankel

August 1972

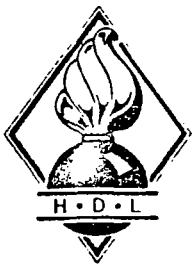

U.S. ARMY MATERIEL COMMAND
HARRY DIAMOND LABORATORIES
WASHINGTON, D.C. 20438

ABSTRACT

This study had two purposes: (1) to assess the relative importance of magnetic and electric coupling parameters of braided shields in the determination of terminal response of braided-shield cables to external electromagnetic fields and (2) to compare a postulated coupling model with those on which various experimental determinations of shielding effectiveness have been based. In the first case, formulas for certain special conditions of wave incidence and sheath-conductor terminations are obtained, but their implications are not explored in detail. These results are only preliminary. In the second case, certain discrepancies among various published methods of measurement and between the measurements and the postulated model were studied.

This report also shows formally how the external-field coupling parameters to each conductor of a multiconductor cable may be determined. A review of earlier work indicated that measurements made in the past have been largely incomplete. In some cases, only the effect of the inductance parameter was measured; in others, the composite effect of both inductive and capacitive coupling was measured, but attributed to inductance only. In either category, this analysis shows that the use of such a limited physical model will generally lead to inaccurate predictions of cable terminal response.

CONTENTS

ABSTRACT..... 3

1. INTRODUCTION..... 7

2. ANALYSIS..... 8

2.1 Current and Charge on Cable Exterior: Surface Electric and Magnetic Intensities.....10

2.1.1 Cable Sheath Grounded at One End.....12
2.1.2 Results for Special Directions of Wave Incidence and Polarization.....14
2.1.3 Cable Sheath Grounded at both Ends.....15
2.1.4 Results for Special Directions of Wave Incidence and Polarization.....16
2.2 Coupling from Outer Sheath to Inner Conductors.....17
2.3 Values of $U_c(\ell)$ and $W_c(\ell)$ for the Special Termination and Excitation Conditions of Section 2.1.....19
2.4 Determination of Coupling Parameters: Shielding Effectiveness.21
2.4.1 Determination of the Coupling Parameters of a Multi-Conductor Cable.....22
2.4.2 Match Terminations: Solutions for Inductive- and Capacitive Coupling Parameters.....24
2.4.3 Short-Circuit Terminations: Solutions for Inductive-Coupling Parameters.....24
2.4.4 Open-Circuit Terminations: Solutions for Capacitive-Coupling Parameters.....26
2.4.5 Discussion.....28
2.5 Review of Published Procedures for Coupling Measurement: Relation to Present Analysis.....28
2.6 Coupling of Coaxial Guides through Small Apertures.....29

3. DISCUSSION OF RESULTS.....35

4. CONCLUSIONS.....36

5. LITERATURE CITED.....37

SYMBOL INDEX.....39

APPENDIXES

A. Cable Sheath Grounded at One End: Derivation of Equations (10)...41
B. Short-Circuit Terminations: Proof that $\underline{I}^o \to \underline{I}^i_c$ for $\ell << \lambda_c$.....44
C. Derivation of Formula for Transfer Impedance for Class II and Class IV Definitions and Measurements (Table I).....45

TABLES

I. Various Definitions and Methods of Measurement: Shielding Effectiveness and Transfer Impedance.....30

FIGURES

1. Cable above ground; (a) longitudinal view; (b) cross-section.... 9
2. $G(\rho)$ versus ρ.....14
3. Basic coaxially-coupled (tri-axial) arrangement for shielding effectiveness measurements.....21
4. Schematic representation of coaxially-excited matched cable.....22

5. Schematic representation of coaxially-excited short-circuited cable.....25
6. Schematic representation of a coaxially-excited open-circuited cable.....27
7. Schematic diagram for definition and measurement of shielding effectiveness.....29
8. Rhomboid with diagonals 2f and 2g replaced by ellipse with semi-axes f and g, respectively.....30
9. Coaxial guides coupled through a small hole in their common wall; (a) longitudinal-section; (b) equivalent circuit.....32
10. Ratio of magnetic to electric polarizability as a function of braid weave angle.....34
11. Ratio of outputs at matched terminals as a function of weave angle.....35

1. INTRODUCTION

When the exterior of a braided-sheath cable is subjected to an electromagnetic field, some energy leaks into the cable and is propagated to the terminations. The mechanisms of penetration are: (1) diffusion of energy through the sheath conductor, and (2) through the small non-conducting gaps in the sheath braid.

Diffusion through a thin, solid, cylindrical conductor has been investigated by Schelknuoff and Odarenko (ref 1) for matched terminations and extended by Zorzy and Muehlberger (ref 2) and by Frankel (ref 3) for arbitrary terminations. Only the magnetic component of the external field can yield a significant response in the interior of a solid shield, because tangential electric field components are largely cancelled by scattering, and the normal electric field component is almost entirely terminated in surface charges. The effect of the penetrated magnetic field can be expressed in terms of a surface-coupling impedance that behaves essentially like an inductive reactance. Combined with the current flowing on the sheath exterior, this reactance may, with the help of the compensation theorem, be treated as an equivalent generator in series with the cable-sheath interior. In the case of the solid sheath, this single inductive parameter is sufficient to quantitatively describe the ability of the external field to penetrate the shield and propagate to the terminations.

Penetration of the external field by way of the braid-air gaps is far more difficult to describe quantitatively, although the basic physical phenomenon has been understood for a long time. Thus Bethe (ref 4) and, more recently, Kaden (ref 5) have calculated the effects of a field penetrating a small circular hole in a plane conducting surface. These studies have been extended to include penetration through small elliptical holes (ref 6) and applied, among other devices, to coupling between coaxial guides (ref 7). Corresponding to penetration by both electric and magnetic fields, an equivalent circuit has been derived

---

[1] Schelkunoff, S.A. and Odarenko, T.M., "Cross-Talk between Coaxial Lines," Bell System Technical Journal, Vol. 16, No. 2, April 1937, pp. 144-164.

[2] Zorzy, J. and Muehlberger, R.F., "RF Leakage Characteristics of Popular Coaxial Cables and Connectors, 500 Mc to 7.5 Gc," Microwave Journal, Vol. 4, No. 11, November 1961, pp. 80-86.

[3] Sidney Frankel & Associates, Menlo Park, California, "Penetration of a Travelling Surface Wave into a Coaxial Cable (First Interim Report)," Sandia Report SC-CR-67-2702, August 1967.

[4] Bethe, H.A., "Theory of Diffraction by Small Holes," Physical Review, Second Series, Vol. 66, No. 7 and 8, October 1 and 15, 1944, pp. 163-182.

[5] Kaden, H., Wirbelstrome und Schirmung in der Nachrichtentechnik, Springer-Verlag, Berlin, 1959.

[6] Montgomery, C.G., Dicke, R.H., and Purcell, E.M., Principles of Microwave Circuits, MIT Radiation Laboratory Series, Vol. 8, McGraw-Hill, New York, 1948.

[7] Marcuvitz, N., Waveguide Handbook, MIT Radiation Laboratory Series, Vol. 10, McGraw-Hill, New York, 1948.

for coupling between coaxial guides through a small elliptical hole, exhibiting both series-reactance coupling and shunt-susceptance coupling (ref 7). Much of this information has been collected and discussed by Vance and Chang (ref 8).

In the case of a braided-sheath cable, the holes are presumed to be rhomboidal in shape and there are many of them (ref 8). Neither penetration through rhomboidal apertures nor the interaction effects of many apertures in close proximity have been theoretically investigated.

Regardless of these considerations, the basic physical fact remains that complete description of the coupling effects generally requires two parameters for a conventional single-wire cable, or two sets of parameters for a multi-wire cable. However, much of the literature seems devoted to the determination of a single parameter: either "shielding effectiveness," which measures a current or power ratio between exterior and interior of the shield; or a "transfer impedance," which is the surface-coupling impedance previously mentioned in connection with solid-shield penetration (ref 2, 8-12).

The purpose of this report is to define a procedure for determining (with the help of certain basic measurements) the terminal response of an N-conductor, braided-sheath cable to an external field for arbitrary terminations. The (2N) coupling parameters required to describe this behavior are not amenable to theoretical determination. Appropriate experimental approaches are implied by the cable theory results obtained. Information pertaining to a model of the coupling phenomena for coaxial guides, taken mainly from Marcuvitz (ref 7) and Vance and Chang (ref 8) is presented in section 2.6. The estimate given here for the inductive-coupling parameter of a simple, coaxial, braided-sheath cable is limited to the effect of aperture coupling only, and therefore is not applicable to the lower frequencies where diffusion coupling is likely to dominate.

2. ANALYSIS

The physical model under investigation is shown schematically in figure 1. An N-conductor cable, ℓ meters long, with sheath outer radius a, is situated at a height h above a perfectly conducting ground. Cable conductors and cable sheath are assumed lossless. The cable dielectric is homogeneous and isotropic. Electric and magnetic fields

[8] Vance, E.F. and Chang, H., "Shielding Effectiveness of Braided-Wire Shields," Technical Memorandum No. 16, AFWL Contract F29601-69-C-0127, November 1971.

[9] Krügel, L., "Shielding Effectiveness of Outer Conductors of Flexible Coaxial Cable," (Abschirmwirkung von Aussenleitern Flexibler Koaxialkable), Telefunken-Zeitung, Vol. 29, December 1936, pp. 256-266.

[10] Osborn, D.C. and Petschek, A.G., "Computer Analysis of Coupling in Braid-Shielded Cable," Systems, Science, and Software Report 3SR-276-1, 8 June 1970, La Jolla, California.

[11] Miller, D.A. and Toulios, P.P., "Penetration of Coaxial Cables by Transient Fields," IEEE EMC Symposium Record, 1968, pp. 414-423.

[12] Knowles, E.D. and Olson, L.W., "Braided Cable Shielding Effectiveness Study," Boeing Company REV LTR, Code Ident. No. 81205, Number T2-3886-1, October 9, 1970.

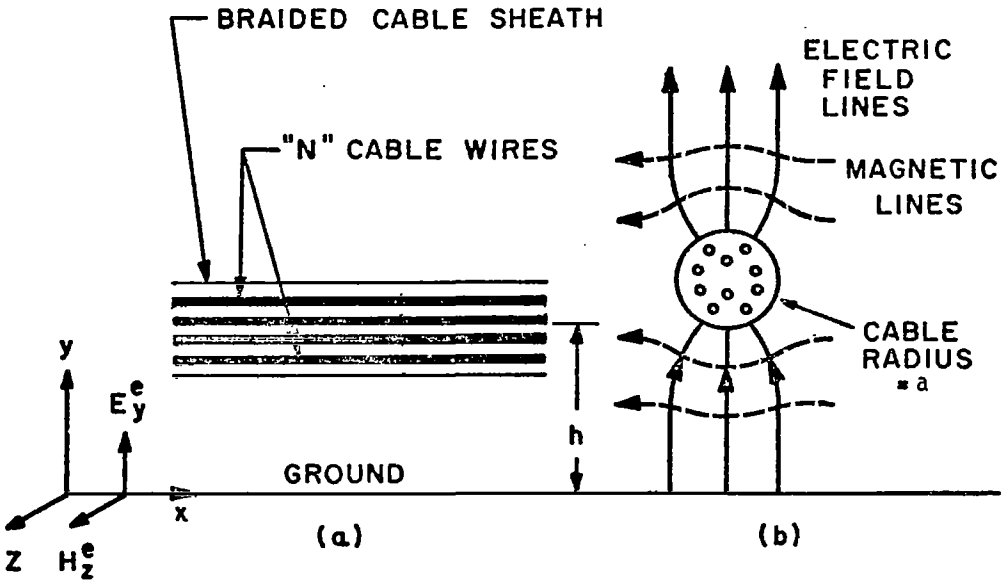

Figure 1. Cable above ground: (a) longitudinal view; (b) cross-section.

$E_y^e(x)$ and $H_z^e(x)$ respectively, are incident on the cable. E_y^e and H_z^e are the fields that would be present if the cable were absent. A component, E_z^i, may also be incident on the cable, but its effect is assumed to be cancelled by the wave reflected from the perfect ground (ref 13). The field, distorted by the cable, is pictured in figure 1(b).

At each hole in the braided sheath, the effects of the external fields are as though electric and magnetic dipoles are present in the plane of the hole (ref 4-6, 8). The fields of these dipoles induce charges on the cable wires and potential differences on the wires with respect to the sheath. Because the geometry is small compared to the wavelength of the impressed field, these couplings may be treated as quasi-static; i.e., magnetic couplings may be characterized as inductances, while the electric couplings are treated as capacitances. Assuming that the sheath has a large number of holes in a cable length much smaller than a wavelength, and that the variance in dipole strengths produced by variations in hole geometries is small enough, we can treat these coupling parameters as continuous and constant along the line. The differential equations describing this situation are formally identical with those treated previously for multiconductor TEM (transverse electromagnetic) lines (ref 14). Solution of the latter problem was relatively simple, largely because of the assumption that strict TEM behavior yields a single propagation mode. In more general

[13] Harrison, C.W., "Bounds on the Load Current of Exposed One- and Two-Conductor Transmission Lines Electromagnetically Coupled to a Rocket," IEEE, Trans. on Electromagnetic Compatability, Vol. EMC-14, No. 1, pp. 4-9, February 1972.

[14] Sidney Frankel & Associates, Menlo Park, California, Interim Report, "Response of a Multiconductor Transmission Line to Excitation by an Arbitrary Monochromatic Impressed Field along the Line," Sandia Report SC-CR-71 5076, April 1971.

situations, such as those involving mixed dielectrics or those involving an upset in the TEM balance between inductive and capacitive couplings--as is generally the case with braided-sheath cables--multiple propagation modes are involved, and consequently the solution tends to be much more complicated.

Fortunately, in the present situation, coupling between inside and outside of the cable sheath is so small that reaction of the inner conductors on the outer region of the sheath may be ignored. In that case, a good approximate solution should result from studying the problem in two parts:

1. Assuming the sheath to be a solid, round conductor, find the current and charge on the cable exterior caused by external field excitation. From a knowledge of these quantities, determine the normal electric and tangential magnetic intensities averaged around the outer periphery of the sheath (sec. 2.2).

2. Assuming that coupling parameters between sheath surface fields and cable inner conductors are known, compute the terminal responses of the cable conductors.

In this report, attention is confined primarily to finding the response of a conventional coaxial cable (single inner conductor). Even for this special case, a theoretical solution for the coupling parameters has not been found. Experimental determination of these parameters is discussed in section 2.4.

2.1 Current and Charge on Cable Exterior: Surface Electric and Magnetic Intensities

We specialize earlier results (ref 14) to a single conductor (the cable sheath exterior) above ground. Let

Z_{0s} = characteristic impedance of cable exterior with respect to ground (Ω)
Y_{0s} = characteristic admittance = Z_{0s}^{-1} ($\mho$)
Y_s^i = cable sheath termination admittance at x = 0 ($\mho$)
Y_s^ℓ = cable sheath termination admittance at x = ℓ ($\mho$)
$V_s(x)$ = cable sheath exterior potential with respect to ground (V)
$I_s(x)$ = cable sheath exterior current (A)
V_s^i, I_s^i = cable sheath exterior potential and current, respectively, at x = 0
V_s^o, I_s^o = cable sheath exterior potential and current, respectively, at x = ℓ
$P_s^i = Y_s^i/Y_{0s} = Z_{0s}Y_s^i$
$P_s^\ell = Y_s^\ell/Y_{0s} = Z_{0s}Y_s^\ell$
β_s = cable sheath exterior phase constant (rad/m)

Define

$$\left.\begin{aligned} S_s &= (P_s^i + P_s^o)\cos\beta_s\ell + j(1 + P_s^oP_s^i)\sin\beta_s\ell \\ K_s(\ell) &= Z_{0s}[W_s(\ell) - Y_s^oU_s(\ell)] \\ U_s(\ell) &= \int_0^\ell \{E_s^e(\xi)\cos[\beta_s(\ell-\xi)] - jZ_{0s}H_s^e(\xi)\sin[\beta_s(\ell-\xi)]\}d\xi \\ W_s(x) &= Y_{0s}\int_0^x \{Z_{0s}H_s^e(\xi)\cos[\beta_s(x-\xi)] - jE_s^e(\xi)\sin[\beta_s(x-\xi)]\}d\xi \\ & \qquad 0 \le x \le \ell \end{aligned}\right\} \quad (1)$$

where $E_s^e(x)$ and $H_s^e(x)$ are distributed equivalent series-voltage and shunt-current sources along the line resulting from the external magnetic and electric fields, respectively.

Then at the sheath terminals (TEM propagation assumed throughout),

$$\left.\begin{aligned} V_s^i &= S_s^{-1}K_s(\ell) \\ V_s^o &= (\cos\beta_s\ell + jP_s^i\sin\beta_s\ell)S_s^{-1}K_s(\ell) + U_s(\ell) \\ I_s^i &= -Y_s^iV_s^i \\ I_s^o &= Y_s^oV_s^o \end{aligned}\right\} \quad (2)$$

At any point x along the sheath (ref 14)

$$I_s(x) = -Y_{0s}(P_s^i\cos\beta_s x + j\sin\beta_s x)S_s^{-1}K_s(\ell) + W_s(x) \quad (3)$$

The various quantities used here are defined and discussed more fully in earlier work (ref 14, 15). For present purposes, the series-voltage and shunt-current sources are defined as

$$\left.\begin{aligned} E_s^e(x) &= j\omega L_s^e H_z^e(x) \\ H_s^e(x) &= j\omega C_s^e E_y^e(x) \end{aligned}\right\} \quad (4)$$

where L_s^e and C_s^e are the external magnetic- and electric-field coupling parameters, respectively (ref 14-16). The electric-field coupling parameter C_s^e in eq 4 is defined as $-C_s^e$ in a previous report (ref 14).

The coupling parameters L_s^e and C_s^e have been determined for a solid sheath cable at arbitrary height above ground (ref 17). Using the same result for the braided sheath, we get

$$\left.\begin{aligned} L_s^e &= \mu_0 h\,\frac{\sqrt{\rho^2-1}}{\rho} \\ C_s^e &= -C_s h\,\frac{\sqrt{\rho^2-1}}{\rho} \end{aligned}\right\} \quad (5)$$

where $\rho = h/a$, C_s is the cable sheath capacitance to ground per meter of line and μ_0 is the magnetic permeability of free space

$$\mu_0 = 4\pi \times 10^{-7}\ \text{H/m}$$

In all cases involving a cable above ground, we will concern ourselves with external fields that behave according to

---

[15]Frankel, S., "TEM Response of a Multiwire Transmission Line (Cable) to an Externally-Impressed Electromagnetic Field: Recipe for Analysis," Harry Diamond Laboratories, Washington, D.C.

[16]Frankel, S., "Externally-Excited Transmission Line: Definition of Procedures for Determining Coupling Parameters," Harry Diamond Laboratories HDL-TM-72-11, April 1972.

[17]Frankel, S., "Field Coupling Parameters for a Single Round Wire Close to a Ground Plane or Two Large Round Wires in Free Space," Harry Diamond Laboratories HDL-TM-72-14, April 1972.

$$\left.\begin{aligned} H_z^e(x) &= H_z^e(0)\exp(-j\beta_e x) \\ E_y^e(x) &= E_y^e(0)\exp(-j\beta_e x) \end{aligned}\right\} \quad (6)$$

where

$$0 \leq \beta_e \leq \beta_s = \frac{\omega}{v_0}$$

and v_0 is the free space velocity of propagation.

In that case, eq 4 becomes

$$\left.\begin{aligned} E_s^e(x) &= E_s^e(0)\exp(-j\beta_e x) \\ H_s^e(x) &= H_s^e(0)\exp(-j\beta_e x) \end{aligned}\right\} \quad (7)$$

and the third and fourth of eq 1 become

$$\left.\begin{aligned} U_s(\ell) &= E_s^e(0)\phi_{s,\ell} - jZ_{0s}H_s^e(0)\psi_{s,\ell} \\ W_s(x) &= H_s^e(0)\phi_{s,x} - jY_{0s}E_s^e(0)\psi_{s,x} \end{aligned}\right\} \quad (8)$$

where for $\beta_s \neq \beta_e$ (for $\beta_s = \beta_e$, see eq 20),

$$\left.\begin{aligned} \phi_{s,x} &= \int_0^x \exp(-j\beta_e\xi)\cos[\beta_s(x-\xi)]d\xi \\ &= (\beta_s^2 - \beta_e^2)^{-1}[j\beta_e\cos\beta_s x + \beta_s\sin\beta_s x - j\beta_e\exp(-j\beta_e x)] \\ \psi_{s,x} &= \int_0^x \exp(-j\beta_e\xi)\sin[\beta_s(x-\xi)]d\xi \\ &= (\beta_s^2 - \beta_e^2)^{-1}[j\beta_e\sin\beta_s x - \beta_s\cos\beta_s x + \beta_s\exp(-j\beta_e x)] \end{aligned}\right\} \quad (9)$$

for $0 \leq x \leq \ell$.

In practice, the cable is situated parallel to the ground at a height varying from zero to that of overhead telephone cables and grounded at one or both ends. The external fields $H_z^e(x)$ and $E_y^e(x)$ induce travelling waves of current and voltage in both directions on the exterior of the cable, and these in turn are associated with a tangential magnetic intensity $H_\phi(x)$ and a normal electric intensity $E_r(x)$ at the exterior surface. These surface fields then couple energy into the interior of the cable through the openings in the braid, as outlined in the introduction. Since there has been some question in the past as to whether the cable sheath should be grounded at one or both ends, both cases are treated here.

2.1.1 Cable Sheath Grounded at One End

With the sheath grounded at $x = 0$ and open-circuited at $x = \ell$, the following expressions for the average magnetic and electric intensities $\overline{H_\phi(x)}$ and $\overline{E_r(x)}$ are derived in appendix A:

$$\left.\begin{aligned}
\overline{H_\phi(x)} &= -\frac{\sec \beta_s \ell}{\eta_0(1-\nu^2)} G(\rho)\Big\{j[E_y^e(0) - \nu\eta_0 H_z^e(0)]\sin[\beta_s(x-\ell)] \\
&\qquad + [\nu E_y^e(0) - \eta_0 H_z^e(0)][\exp(-j\beta_e x)\cos\beta_s\ell - \exp(-j\beta_e\ell)\cos\beta_s x]\Big\} \\
\overline{E_r(x)} &= \frac{\sec \beta_s \ell}{1-\nu^2} G(\rho)\Big\{[E_y^e(0) - \nu\eta_0 H_z^e(0)]\cos[\beta_s(x-\ell)] \\
&\qquad - [\nu E_y^e(0) - \eta_0 H_z^e(0)][\nu\exp(-j\beta_e x)\cos\beta_s\ell + j\exp(-j\beta_e\ell)\sin\beta_s x]\Big\}
\end{aligned}\right\} \quad (10)$$

$0 \le x \le \ell;\ 0 \le \nu < 1$

where η_0 is the free-space wave impedance

$$\eta_0 = \sqrt{\mu_0/\varepsilon_0} \quad (11)$$

ε_0 is the free-space dielectric permittivity

$$\varepsilon_0 = \frac{10^{-9}}{36\pi} \text{ F/m}$$

$$\nu = \beta_e/\beta_s;\ 0 \le \nu < 1 \quad (12)$$

and

$$G(\rho) = \frac{\sqrt{\rho^2-1}}{\cosh^{-1}\rho};\quad \rho = h/a \quad (13)$$

Eq 10 are unsuitable for analysis under certain conditions of interest. For instance, when $\beta_s\ell$ is an odd multiple of $\pi/2$, eq 10 becomes infinite. In actual fact, the peak values are limited by sheath, ground, and small radiation losses. These are adequately taken into account by replacing $j\beta_s$ with

$$\gamma_s = \alpha_s + j\beta_s \quad (14)$$

where α_s is the exterior line attenuation constant in nepers/meter. In that case, the singular factor $\sec \beta_s\ell$ is replaced by $\operatorname{sech} \gamma_s\ell$ which at

$$\beta_s\ell = (2m+1)\frac{\pi}{2};\ m = \text{Integer}$$

becomes

$$\operatorname{sech} \gamma_s\ell \to (-1)^m j\operatorname{csch} \alpha_s\ell \quad (15)$$

Another instance of difficulty occurs when $\nu = 1$. This case is treated later in this section.

$G(\rho)$, defined in eq 13, is the only factor in eq 10 representing their behavior as a function of ρ, and is common to both $\overline{H_\phi}$ and $\overline{E_r}$ in such a way that their relative values are independent of ρ. $G(\rho)$ is plotted in figure 2. As $\rho \to 1$, $G \to 1$, while for large ρ, the asymptotic behavior of G is

$$G \to \frac{\rho}{\ell n\,(2\rho)} \text{ as } \rho \to \infty \quad (16)$$

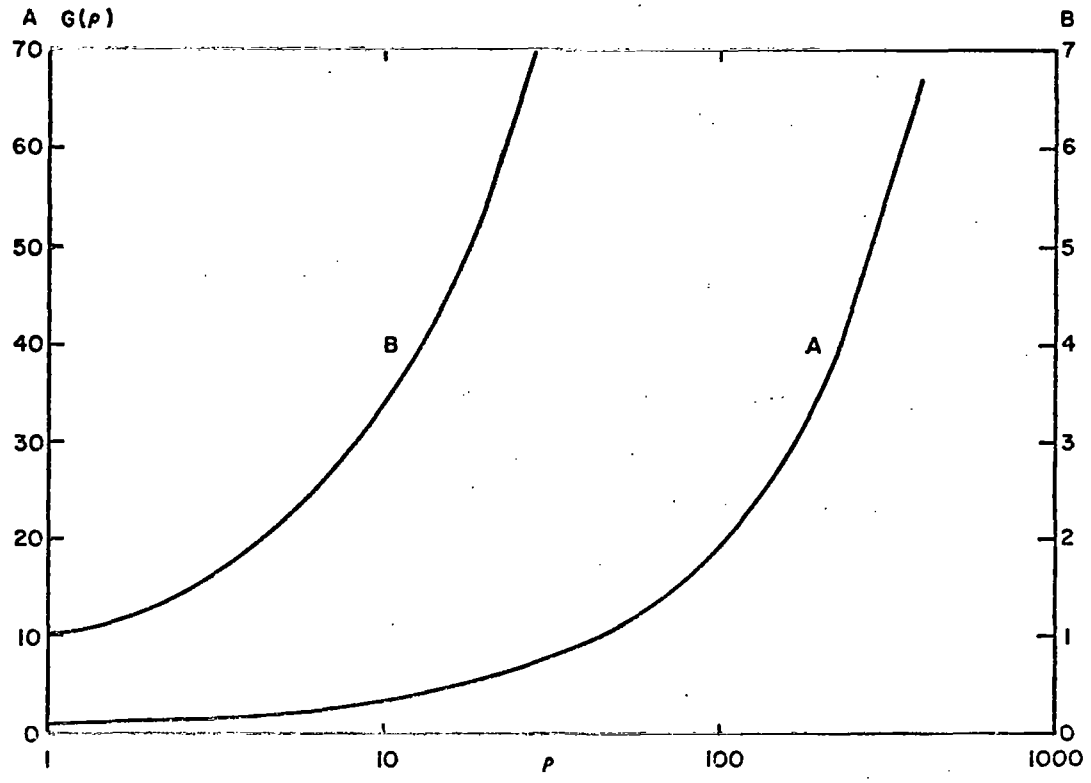

Figure 2. G(ρ) versus ρ.

2.1.2 Results for Special Directions of Wave Incidence and Polarization

We consider two cases of special interest: (1) horizontally polarized wave, plane of incidence coincident with cable's transverse plane; and (2) vertically polarized travelling wave, direction parallel to cable axis. For the first case, we have $E_y^e \equiv 0$, $H_z^e \neq$ constant, and furthermore, $\beta_e = 0$. Hence, $\nu = 0$, and eq 10 reduces to

$$\left.\begin{aligned} \overline{H_\phi(x)} &= G(\rho)H_z^e[1 - (\sec \beta_s \ell)(\cos \beta_s x)] \\ \overline{E_r(x)} &= j\eta_0 G(\rho)H_z^e(\sec \beta_s \ell)(\sin \beta_s x) \end{aligned}\right\} \quad (17)$$

In the second case, we have the incident wave travelling in the positive direction, so that $\beta_e = \beta_s$ ($\nu = 1$), and furthermore

$$\frac{E_y^e(x)}{H_z^e(x)} = \eta_0 \quad (18)$$

As a consequence of eq 18, eq A-13 of appendix A yields

$$H_s^e(0) + Y_{0s}E_s^e(0) = 0 \quad (19)$$

Substitution of these conditions in eq 10 leads to indeterminate results for $\bar{H}_\phi$ and $\bar{E}_r$. However, these indeterminacies may be resolved by apply L-Hospital's rule to eq 9 and A-8. We get

$$\left.\begin{aligned}
\lim_{\beta_e\to\beta_s} \phi_{s,x} &= \frac{\sin\beta_s x + (\beta_s x)\exp(-j\beta_s x)}{2\beta_s} \\
\lim_{\beta_e\to\beta_s} \psi_{s,x} &= -j\left[\frac{\sin\beta_s x - (\beta_s x)\exp(-j\beta_s x)}{2\beta_s}\right] \\
\lim_{\beta_e\to\beta_s} \left(\frac{d\phi_{s,x}}{dx}\right) &= \frac{1}{2}\left[2\cos\beta_s x - j\sin\beta_s x - j(\beta_s x)\exp(-j\beta_s x)\right] \\
\lim_{\beta_e\to\beta_s} \left(\frac{d\psi_{s,x}}{dx}\right) &= \frac{1}{2}\left[\sin\beta_s x + (\beta_s x)\exp(-j\beta_s x)\right]
\end{aligned}\right\} \quad (20)$$

Then, using these in eq 8 and A-7, and then in eq A-6, there replacing $Y_{0s}E_s^e(0)$ through eq 19 and finally replacing $H_s^e(0)$ through A-12 yields

$$\left.\begin{aligned}
\overline{H_\phi(x)} &= -jG(\rho)\frac{E_y^e(0)}{\eta_0}\left[(\sec\beta_s\ell)\right]\sin[\beta_s(x-\ell)] \\
\overline{E_r(x)} &= G(\rho)E_y^e(0)[\sec\beta_s\ell]\cos[\beta_s(x-\ell)]
\end{aligned}\right\} \quad (21)$$

Alternatively, these may be written, from eq 18 as

$$\left.\begin{aligned}
\overline{H_\phi(x)} &= -jG(\rho)H_z^e(0)[\sec\beta_s\ell]\sin[\beta_s(x-\ell)] \\
\overline{E_r(x)} &= G(\rho)\eta_0 H_z^e(0)[\sec\beta_s\ell]\cos[\beta_s(x-\ell)]
\end{aligned}\right\} \quad (22)$$

2.1.3 Cable Sheath Grounded at Both Ends

We have

$$P_s^I = P_s^o \to \infty$$

$$S_s \to jP_s^oP_s^I\sin\beta_s\ell \quad \text{(eq 1)}$$

$$K_s(\ell) \to -P_s^oU_s(\ell) \quad \text{(eq 1)}$$

Eq 3 becomes

$$I_s(x) = W_s(x) - jY_{0s}U_s(\ell)(\csc\beta_s\ell)(\cos\beta_s x) \quad (23)$$

and we get

$$\frac{dI_s}{dx} = \frac{dW_s}{dx} + j\beta_s Y_{0s}U_s(\ell)(\csc\beta_s\ell)(\sin\beta_s x) \quad (24)$$

For the exterior sheath surface fields we get from eq A-3 and A-4 of appendix A

$$\left.\begin{aligned}\overline{H_\phi(x)} &= \frac{\csc \beta_s \ell}{2\pi a}\left[W_s(x)\sin \beta_s \ell - jY_{0s}U_s(\ell)\cos \beta_s x\right] \\ \overline{E_r(x)} &= -\frac{\csc \beta_s \ell}{j2\pi a\varepsilon_0\omega}\left[\frac{dW_s}{dx}\sin \beta_s \ell + j\beta_s Y_{0s}U_s(\ell)\sin \beta_s x\right]\end{aligned}\right\} \quad (25)$$

Following the same procedures as in the previous case, we get

$$\left.\begin{aligned}\overline{H_\phi(x)} &= -\frac{\csc \beta_s \ell}{\eta_0(1-\nu^2)}G(\rho)\Big\{j[E_y^e(0) - \nu\eta_0 H_z^e(0)][\cos \beta_s(x-\ell) - \exp(-j\beta_e \ell)\cos \beta_s x] \\ &\quad + [\nu E_y^e(0) - \eta_0 H_z^e(0)]\exp(-j\beta_e x)\sin \beta_s \ell\Big\} \\ \overline{E_r(x)} &= -\frac{\csc \beta_s \ell}{1-\nu^2}G(\rho)\Big\{[E_y^e(0) - \nu\eta_0 H_z^e(0)][\sin \beta_s(x-\ell) + \exp(-j\beta_e \ell)\sin \beta_s x] \\ &\quad + \nu[\nu E_y^e(0) - \eta_0 H_z^e(0)]\exp(-j\beta_s x)\sin \beta_s \ell\Big\}\end{aligned}\right\} \quad (26)$$

for $0 \leq x \leq \ell$; $0 \leq \nu < 1$.

In eq 26, infinite resonance effects are exhibited for $\beta_s \ell = m\pi$, m integer, as in section 2.1.1, the remedy is to replace $j\beta_s$ with γ_s (eq 14). In that case, csc $\beta_s \ell$ is replaced by jcsch $\gamma_s \ell$ which at

$$\beta_s \ell = m\pi$$

becomes

$$j\operatorname{csch} \gamma_s \ell \to (-1)^m j\operatorname{csch} \alpha_s \ell \quad (27)$$

2.1.4 Results for Special Directions of Wave Incidence and Polarization

Again, we consider two special cases. First, in the case of a horizontally polarized wave for which the plane of incidence is coincident with the cable's transverse plane, $E_y^e = 0$, H_z^e = constant, and $\beta_e = 0$; hence, $\nu = 0$ and eq 26 becomes

$$\left.\begin{aligned}\overline{H_\phi(x)} &= -G(\rho)H_z^e \\ \overline{E_r(x)} &\equiv 0\end{aligned}\right\} \quad (28)$$

In this particular case, coupling into the cable depends only on the current flowing on the sheath exterior.

Second, in the case of a vertically polarized travelling wave where the direction of propagation is parallel to the cable axis, $\beta_e = \beta_s$, $\nu = 1$, and eq 18 holds. Eq 26 are indeterminate. Proceeding as in the corresponding situation with the cable grounded at one end, we get

$$\left.\begin{aligned}\overline{H_\phi(x)} &= G(\rho)\frac{E_y^e(0)}{\eta_0}\exp(-j\beta_s x) \\ \overline{E_r(x)} &= G(\rho)E_y^e(0)\exp(-j\beta_s x)\end{aligned}\right\} \quad (29)$$

2.2 Coupling from Outer Sheath to Inner Conductors

In section 2.1, we derived expressions for the electric and magnetic intensities at the outer surface of a braided shield above perfect ground (by treating it as a solid cylindrical conductor) for various cable terminations and impressed fields.

As explained in the introduction, the existence of many small openings in the braided shield permits penetration of fractions of both electric and magnetic intensities to the interior of the cable. A semi-quantitative discussion of the physical nature of these couplings will be discussed in section 2.6. In this section, we treat the problem formally, assuming that the parameters linking external surface field strengths to cable response are known.

Because of the penetration described above, the conductors in the interior of the cable are excited by transverse electric and magnetic fields. The situation is similar to that analyzed previously (ref 14) with certain exceptions that will now be explained. The applied fields are not uniform at any cross-section as previously assumed; first, they are not impressed continuously, but rather at discrete points. However, these are closely spaced compared to an increment of length which is small compared to any wavelength of interest. In other words, there are many discrete sources in a length increment small enough to be treated as a differential element. Mathematically, this is equivalent to a continuous, constant-density source, provided the variance in the geometry and linear density of the holes is small. Second, the discrete source strengths are unequal at any cable cross-section, because the exterior surface field strengths generally vary around the periphery of the sheath. However, we again assume that a sufficient number of discrete sources are distributed around the periphery in any differential element, and especially that the bundle of cable conductors is constructed with a sufficiently high rate of twist so that the summation of the effects of such sources in any differential element is as though they were uniform around the periphery and therefore proportional to the average peripheral fields derived in section 2.1. If the bundle twist does not exist, then coupling parameters must be determined in terms of the point-by-point distribution of the peripheral fields at any cross-section and the orientation of the cable conductors with regard to the external field.

With these provisos, the matrix differential equations and the consequent matrix solutions for the terminal currents apply formally in the present instance. We do not know--and there is little likelihood that we can determine analytically--the impressed fields experienced directly by the cable conductors. However, the coupling parameters between the exterior surface fields and the inner configuration can, in principle, be measured (sec. 2.4), and this should be adequate, along with formal line theory, for predicting the terminal cable response.

Accordingly, we take the external applied fields to be the average intensities, $\overline{H_\phi(x)}$ and $\overline{E_r(x)}$ derived in section 2.1. The results to be stated are a generalization of eq 2 to a system of N conductors within the sheath.

Take the interior of the cable sheath to be the voltage-reference conductor. Let (ref 14-16)

$\underline{Z}$ = cable characteristic impedance matrix (Ω)
= $[Z_{ij}]$, i, j ≡ 1,...,N

$\underline{Y}$ = cable characteristic admittance matrix ($\mho$)
= $[Y_{ij}]$, i, j = 1,...,N
= $\underline{Z}^{-1}$

$\underline{Y}_c^i$ = cable termination matrix at x = 0 ($\mho$)
= $[Y^i_{c,ij}]$, i, j, = 1,...,N (index range applied to subscripts i and j only)

$\underline{Y}_c^o$ = cable termination matrix at x = ℓ ($\mho$)
= $[Y^o_{c,ij}]$, i, j = 1,...,N

$\underline{V}_c^i$, $\underline{I}_c^i$ = cable interior potential and current column vectors respectively, at x = 0 (V), (A)
= $[V^i_{c,i}]$, $[I^i_{c,i}]$, i = 1,...,N

$\underline{V}_c^o$, $\underline{I}_c^o$ = cable interior potential and current column vectors respectively, at x = ℓ (V), (A)
= $[V^o_{c,i}]$, $[I^o_{c,i}]$, i = 1,...,N

$\underline{P}_c^i$ = normalized load admittance matrix at x = 0
= $\underline{Z}\underline{Y}_c^i$

$\underline{P}_c^o$ = normalized load admittance matrix at x = ℓ
= $\underline{Z}\underline{Y}_c^o$

β_c = cable interior phase constant (rad/m)

$\underline{I}$ = N × N unit matrix

$$\left.\begin{aligned}
\underline{S}_c &= (\underline{P}_c^i + \underline{P}_c^o)\cos\beta_c\ell + j(\underline{I} + \underline{P}_c^o\underline{P}_c^i)\sin\beta_c\ell \\
\underline{K}_c(\ell) &= \underline{Z}\,\underline{W}_c(\ell) - \underline{P}_c^o\,\underline{U}_c(\ell) \\
\underline{U}_c(\ell) &= \int_0^\ell \{\underline{E}_c^e(\xi)\cos[\beta_c(\ell-\xi)] - j\underline{Z}\,\underline{H}_c^e(\xi)\sin[\beta_c(\ell-\xi)]\}d\xi \\
\underline{W}_c(\ell) &= \underline{Y}\int_0^\ell \{\underline{Z}\,\underline{H}_c^e(\xi)\cos[\beta_c(\ell-\xi)] - j\underline{E}_c^e(\xi)\sin[\beta_c(\ell-\xi)]\}d\xi
\end{aligned}\right\} \quad (30)$$

where $\underline{E}_c^e(x)$ and $\underline{H}_c^e(x)$ are distributed equivalent series-voltage and shunt-current column vector sources along the cable resulting from the average exterior surface magnetic and electric intensities, respectively (see eq 32 below). Then, at the cable terminals

$$\left.\begin{aligned}
\underline{V}_c^i &= \underline{S}_c^{-1}\underline{K}_c(\ell) \\
\underline{V}_c^o &= (\underline{I}\cos\beta_c\ell + j\underline{P}_c^i\sin\beta_c\ell)\underline{S}_c^{-1}\underline{K}_c(\ell) + \underline{U}_c(\ell) \\
\underline{I}_c^i &= -\underline{Y}_c^i\,\underline{V}_c^i = -\underline{Y}_c^i\,\underline{S}_c^{-1}\underline{K}_c(\ell) \\
\underline{I}_c^o &= \underline{Y}_c^o\,\underline{V}_c^o \\
&= -\underline{Y}[\underline{P}_c^i\cos\beta_c\ell + j\underline{I}\sin\beta_c\ell]\underline{S}_c^{-1}\underline{K}_c(\ell) + \underline{W}_c(\ell)
\end{aligned}\right\} \quad (31)$$

Furthermore (ref 14)

$$E_c^e(x) = j\omega \underline{L}_c^e \overline{H_\phi(x)}$$
$$H_c^e(x) = j\omega \underline{C}_c^e \overline{E_r(x)} \qquad (32)$$

where $\overline{H_\phi(x)}$ and $\overline{E_r(x)}$ are the average intensities at the sheath outer surface computed as in section 2.1. The field coupling-parameter column vectors

$$\left.\begin{aligned} \underline{L}_c^e &= \begin{bmatrix} L_{c,1}^e \\ L_{c,2}^e \\ \cdot \\ \cdot \\ \cdot \\ L_{c,N}^e \end{bmatrix} \\ \underline{C}_c^e &= \begin{bmatrix} C_{c,1}^e \\ C_{c,2}^e \\ \cdot \\ \cdot \\ \cdot \\ C_{c,N}^e \end{bmatrix} \end{aligned}\right\} \qquad (33)$$

must be determined experimentally, perhaps by methods suggested by the theory in section 2.4. Determination of the elements of the cable characteristic impedance/admittance matrix is discussed by Uchida (ref 18).

2.3 Values of $U_c(\ell)$ and $W_c(\ell)$ for Special Termination and Excitation Conditions

The third and fourth of eq 30 have been evaluated for the special conditions considered in sections 2.1. The results are recorded here for future reference.

Case 1: Cable sheath grounded at one end

a. Horizontally polarized wave, plane of incidence coincident with cable's transverse plane.

[18] Uchida, Hidenari, Fundamentals of Coupled Lines and Multi-Wire Antennas, Sasaki Publishing Co., Sendai, Japan, 1967.

$$\underline{U}_c(\ell) = j\omega G(\rho)H_z^e(0)\left\{\frac{\sin \beta_c \ell}{\beta_c}\underline{L}_c^e + \frac{\sec \beta_s \ell}{\beta_c^2 - \beta_s^2}[(\beta_s \sin \beta_s \ell - \beta_c \sin \beta_c \ell)\underline{L}_c^e + \eta_0(\beta_c \sin \beta_s \ell - \beta_s \sin \beta_c \ell)\underline{\underline{Z}}\underline{C}_c^e]\right\} \quad (34a)$$

$$\underline{W}_c(\ell) = \omega G(\rho)H_z^e(0)\left\{\frac{1 - \cos \beta_c \ell}{\beta_c}\underline{\underline{Y}}\underline{L}_c^e - \frac{\sec \beta_s \ell}{\beta_c^2 - \beta_s^2}(\cos \beta_s \ell - \cos \beta_c \ell)(\eta_0 \beta_s \underline{C}_c^e + \beta_c \underline{\underline{Y}}\underline{L}_c^e)\right\} \quad (34b)$$

b. Vertically polarized wave, direction of travel parallel to cable axis.

$$\underline{U}_c(\ell) = \frac{\omega G(\rho)H_z^e(0)\sec \beta_s \ell}{\beta_c^2 - \beta_s^2}\{[\beta_s(1 - \cos \beta_s \ell \cos \beta_c \ell) - \beta_c \sin \beta_s \ell \sin \beta_c \ell]\underline{L}^e + \eta_0[\beta_c(1 - \cos \beta_s \ell \cos \beta_c \ell) - \beta_s \sin \beta_s \ell \sin \beta_c \ell]\underline{\underline{Z}}\underline{C}_c^e\} \quad (35a)$$

$$\underline{W}_c(\ell) = \frac{-j\omega G(\rho)H_z(0)\sec \beta_s \ell}{\beta_c^2 - \beta_s^2}\{(\beta_c \sin \beta_s \ell \cos \beta_c \ell - \beta_s \cos \beta_s \ell \sin \beta_c \ell)\underline{\underline{Y}}\underline{L}_c^e + \eta_0(\beta_s \sin \beta_s \ell \cos \beta_c \ell - \beta_c \cos \beta_s \ell \sin \beta_c \ell)\underline{C}_c^e\} \quad (35b)$$

Case 2: Cable sheath grounded at both ends

a. Horizontally polarized wave, plane of incidence coincident with cable's transverse plane.

$$\underline{U}_c(\ell) = -j\omega G(\rho)H_z^e(0)\frac{\sin \beta_c \ell}{\beta_c}\underline{L}_c^e \quad (36a)$$

$$\underline{W}_c(\ell) = -\omega G(\rho)H_z^e(0)\frac{1 - \cos \beta_c \ell}{\beta_c}\underline{\underline{Y}}\underline{L}_c^e \quad (36b)$$

b. Vertically polarized wave, direction of travel parallel to cable axis.

$$\underline{U}_c(\ell) = \frac{\omega G(\rho)H_z^e(0)}{\beta_c^2 - \beta_s^2}\left(\{\beta_s[\exp(-j\beta_s \ell) - \cos \beta_c \ell] + j\beta_c \sin \beta_c \ell\}\underline{L}_c^e + \eta_0\{\beta_c[\exp(-j\beta_s \ell) - \cos \beta_c \ell] + j\beta_s \sin \beta_c \ell\}\underline{\underline{Z}}\underline{C}_c^e\right) \quad (37a)$$

$$\underline{W}_c(\ell) = \frac{\omega G(\rho)H_z^e(0)}{\beta_c^2 - \beta_s^2}\left(\{\beta_c[\exp(-j\beta_s \ell) - \cos \beta_c \ell] + j\beta_s \sin \beta_c \ell\}\underline{\underline{Y}}\underline{L}_c^e + \eta_0\{\beta_s[\exp(-j\beta_s \ell) - \cos \beta_c \ell] + j\beta_c \sin \beta_c \ell\}\underline{C}_c^e\right) \quad (37b)$$

2.4 Determination of Coupling Parameters: Shielding Effectiveness

Measurement of the penetration of an external electromagnetic field in a braided sheath has usually been based on some variant of a basic tri-axial arrangement as shown in figure 3. In that figure, the outer larger cylinder is the outer conductor of one coaxial line; the axial line segment represents the N inner conductors of the cable, and the central conductor, shown in the form of wiggly lines, represents the braided sheath, its outer surface being the inner conductor of the outer coax, while its inner surface is the outer conductor of the inner cable. Four boxes are shown as unspecified terminations to allow for the necessary flexibility in discussion.

In the various experiments discussed in section 2.5 of this report, N = 1. In all experiments, one coaxial is the driven line, the other, the receiver. Workers have sometimes reported generator and detector to be at the same end of the configuration, and sometimes at opposite ends. Sometimes the outer line is the driven line, sometimes the inner. Values of passive terminations are also mixed, from open circuits to matched impedances to shorts. Whenever possible, the length of the configuration is kept electrically short to simplify analysis.

Here, we are concerned with two questions:

1. What sort of measurements can be made, at least in principle, to determine the coupling parameters $\underline{L}_c^e$ and $\underline{C}_c^e$ (eq 33) of a multiwire cable?

2. How do the coupling parameters developed here enter into measurements previously reported in the literature?

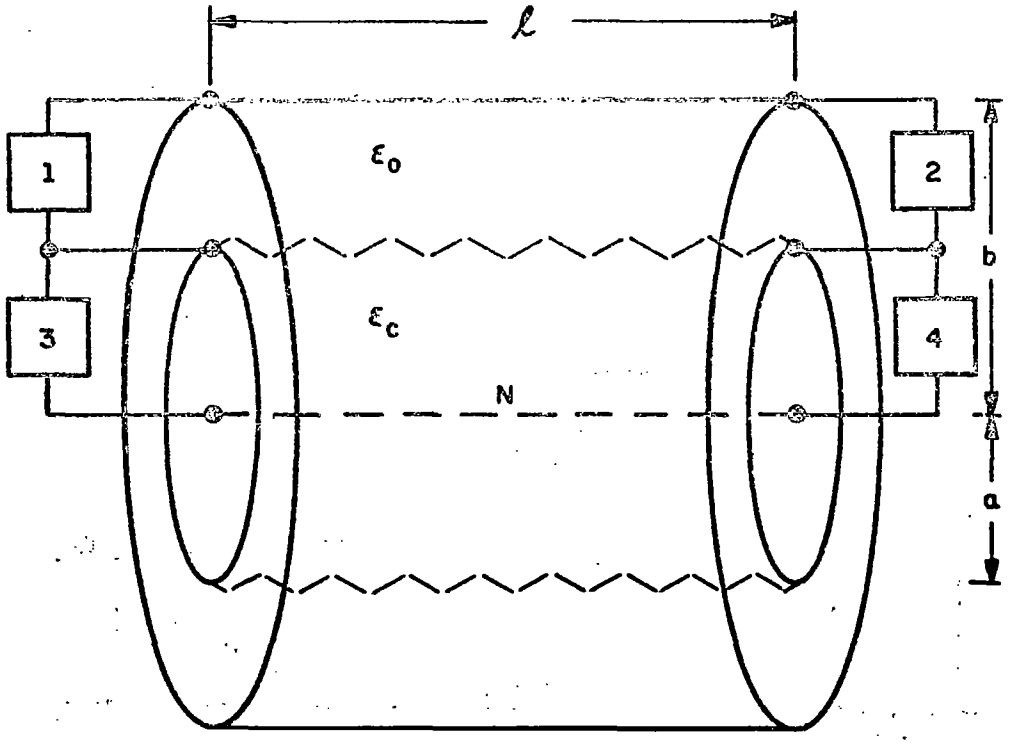

Figure 3. Basic coaxially-coupled (tri-axial) arrangement for shielding-effectiveness measurements.

2.4.1 Determination of the Coupling Parameters of a Multi-Conductor Cable

In figure 3, we assume that the outer coax is excited by a source, either of constant voltage V_g, or of constant current I_g. The cable under test consists of N conductors embedded in a uniform dielectric surrounded by a sheath of outer radius a.

We consider three cases:

1. All passive terminals in both regions are match-terminated.
2. All passive terminals in both regions are terminated in short-circuits.
3. All passive terminals in both regions are terminated in open circuits.

In the second and third cases, we shall assume at the outset that the system is electrically short ($\ell << \lambda_c$, where λ_c is the wavelength in the cable) $\lambda_c \leq \lambda_0$ and λ_0 is the free-space wavelength. In the first case, we derive the results for arbitrary ℓ, and then specialize to small ℓ.

2.4.2 Match Terminations: Solutions for Inductive- and Capacitive Coupling Parameters

Figure 4 is a schematic representation of figure 3 with appropriate terminations. In the outer region, we have, at any point x along the system,

$$\left.\begin{aligned} V_s &= V_g \exp(-j\beta_s x) \\ I_s &= I_g \exp(-j\beta_s x) = Y_{0s} V_g \exp(-j\beta_s x) \end{aligned}\right\} \quad (38)$$

The sheath surface fields are constant around the periphery of a fixed cross-section, so we have

$$\left.\begin{aligned} \overline{H_\phi(x)} = H_\phi(x) &= \frac{-I_s}{2\pi a} = \frac{-I_g}{2\pi a} \exp(-j\beta_s x) = -\frac{Y_{0s} V_g \exp(-j\beta_s x)}{2\pi a} \\ \overline{E_r(x)} = E_r(x) &= \eta_0 H_\phi(x) = \frac{-\eta_0}{2\pi a} Y_{0s} V_g \exp(-j\beta_s x) \end{aligned}\right\} \quad (39)$$

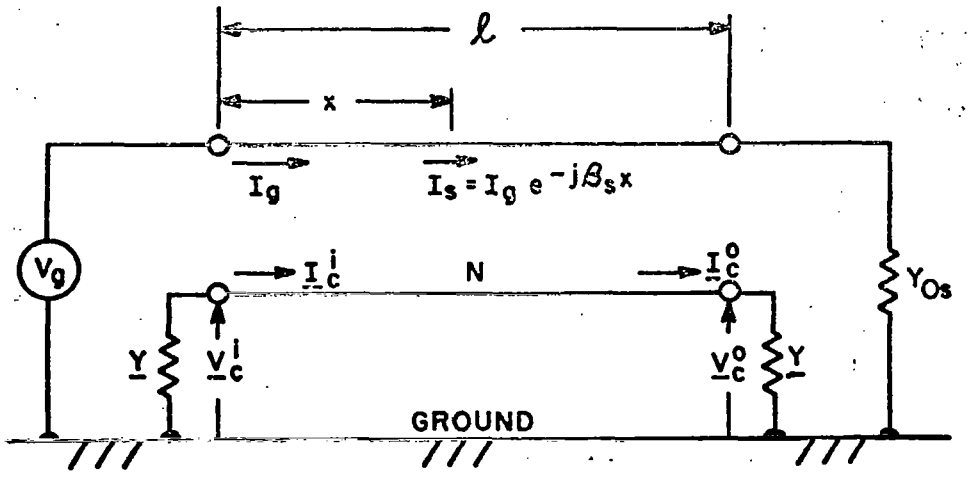

Figure 4. Schematic representation of coaxially-excited matched cable.

For eq 30-32, we have

$$\left.\begin{aligned}
\underline{P}_c^i &= \underline{P}_c^o = \underline{I} \\
\underline{S}_c &= 2\exp(j\beta_c \ell) \\
\underline{E}_c^e(x) &= -\frac{j\omega I_g}{2\pi a}\exp(-j\beta_s x)\underline{L}_c^e \\
\underline{H}_c^e(x) &= -\frac{j\omega\eta_0 I_g}{2\pi a}\exp(-j\beta_s x)\underline{C}_c^e \\
\underline{U}_c(\ell) &= -\frac{j\omega I_g \phi_{c,\ell}}{2\pi a}\underline{L}_c^e - \frac{\omega\eta_0 I_g \psi_{c,\ell}}{2\pi a}\underline{ZC}_c^e \\
\underline{ZW}_c(\ell) &= -\frac{j\omega\eta_0 I_g \phi_{c,\ell}}{2\pi a}\underline{ZC}_c^e - \frac{\omega I_g \psi_{c,\ell}}{2\pi a}\underline{L}_c^e \\
\underline{K}_c(\ell) &= \underline{ZW}_c(\ell) - \underline{U}_c(\ell) \\
&= \frac{j\omega I_g}{2\pi a}(\underline{L}_c^e - \eta_0 \underline{ZC}_c^e)(\phi_{c,\ell} + j\psi_{c,\ell})
\end{aligned}\right\} \quad (40)$$

$$\left.\begin{aligned}
\phi_{c,\ell} &= \frac{j\beta_s \cos\beta_c\ell + \beta_c \sin\beta_c\ell - j\beta_s\exp(-j\beta_s\ell)}{\beta_c^2 - \beta_s^2} \\
\psi_{c,\ell} &= \frac{j\beta_s \sin\beta_c\ell - \beta_c\cos\beta_c\ell + \beta_c\exp(-j\beta_s\ell)}{\beta_c^2 - \beta_s^2}
\end{aligned}\right\} \quad (41)$$

by analogy with eq 9. From eq 41,

$$\phi_{c,\ell} + j\psi_{c,\ell} = \frac{\exp(j\beta_c\ell) - \exp(-j\beta_s\ell)}{j(\beta_c + \beta_s)} \quad (42)$$

so the last of eq 40 becomes

$$\underline{K}_c(\ell) = \frac{\omega I_g}{2\pi a}\frac{\exp(j\beta_c\ell) - \exp(-j\beta_s\ell)}{\beta_c + \beta_s}(\underline{L}_c^e - \eta_0\underline{ZC}_c^e) \quad (43)$$

Using these results in eq 31,

$$\underline{V}_c^i = \frac{\omega I_g}{2\pi a}\frac{1 - \exp[-j(\beta_c + \beta_s)\ell]}{\beta_c + \beta_s}(\underline{L}_c^e - \eta_0\underline{ZC}_c^e) \quad (44a)$$

$$\begin{aligned}
\underline{V}_c^o &= \exp(j\beta_c\ell)\underline{V}_c^i + \underline{U}_c(\ell) \\
&= \tfrac{1}{2}\underline{K}_c(\ell) + \underline{U}_c(\ell) \\
&= -\frac{j\omega I_g}{4\pi a}(\phi_{c,\ell} - j\psi_{c,\ell})(\underline{L}_c^e + \eta_0\underline{ZC}_c^e) \\
&= \frac{\omega I_g}{4\pi a}\frac{\exp(-j\beta_c\ell) - \exp(-j\beta_s\ell)}{\beta_c - \beta_s}(\underline{L}_c^e + \eta_0\underline{ZC}_c^e)
\end{aligned} \quad (44b)$$

Eq 44 may be solved simultaneously for $\underline{L}_c^e$ and $\underline{C}_c^e$:

$$\left.\begin{aligned}\underline{L}_c^e &= \frac{2\pi a}{\omega I_g}\left\{\frac{\beta_c - \beta_s}{\exp(-j\beta_c \ell) - \exp(-j\beta_s \ell)}\,\underline{V}_c^o + \frac{\beta_c + \beta_s}{1 - \exp[-j(\beta_c + \beta_s)\ell]}\,\underline{V}_c^i\right\}\\ \underline{C}_c^e &= \frac{2\pi a}{\eta_0 \omega I_g}\left\{\frac{\beta_c - \beta_s}{\exp(-j\beta_c \ell) - \exp(-j\beta_s \ell)}\,\underline{I}_c^o + \frac{\beta_c + \beta_s}{1 - \exp[-j(\beta_c + \beta_s)\ell]}\,\underline{I}_c^i\right\}\end{aligned}\right\} \quad (45)$$

where

$$\left.\begin{aligned}\underline{I}_c^i &= -\underline{Y}\underline{V}_c^i\\ \underline{I}_c^o &= \underline{Y}\underline{V}_c^o\end{aligned}\right\} \quad (46)$$

For $\ell << \lambda_c$, eq 46 becomes

$$\left.\begin{aligned}\underline{L}_c^e &= \frac{2\pi a}{j\omega I_g \ell}\,(\underline{V}_c^i - \underline{V}_c^o)\\ \underline{C}_c^e &= \frac{2\pi a}{j\omega \eta_0 I_g \ell}\,(\underline{I}_c^i - \underline{I}_c^o)\end{aligned}\right\} \quad (47)$$

Eq 47 suggests a procedure on which determination of $\underline{L}_c^e$ and $\underline{C}_c^e$ can be based. Current and voltage phase angles must be watched carefully (note also, eq 46), although it is clear that, for $\ell << \lambda_0$, phase angles can differ only by zero or π.

2.4.3 Short-Circuit Terminations: Solutions for Inductive-Coupling Parameters

The schematic is shown in figure 5. We start with the assumption that $\ell << \lambda_c$, so that we can take

$$\left.\begin{aligned}\overline{H}_\phi &= \text{constant} = \frac{-I_g}{2\pi a}\\ \overline{E}_r &\equiv 0\end{aligned}\right\} \quad (48)$$

Then, from eq 32

$$\left.\begin{aligned}\underline{E}_c^e &= -\frac{j\omega I_g}{2\pi a}\,\underline{L}_c^e\\ \underline{H}_c^e &= 0\end{aligned}\right\} \quad (49)$$

Short-circuit terminations imply that $\underline{p}_c^i$, $\underline{p}_c^o \to \infty$. To assure that they do so independently, we take

$$\left.\begin{aligned}\underline{P}_c^i &= k^i \underline{P}\\ \underline{P}_c^o &= k^o \underline{P}\end{aligned}\right\} \quad (50)$$

where k^i and k^o are arbitrary scalar constants different from zero and $\underline{P} \to \infty$. We have

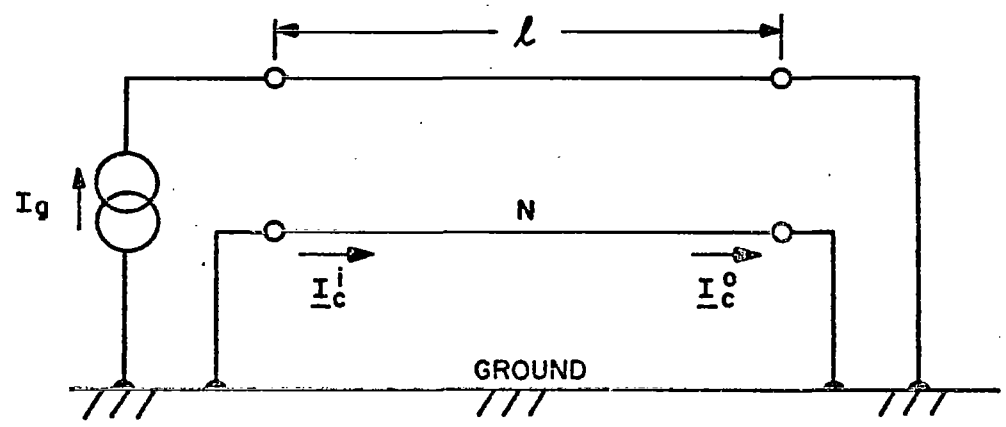

Figure 5. Schematic representation of coaxially-excited open-circuited cable.

$$\left.\begin{aligned} \underline{U}_c(\ell) &= \underline{E}_c^e \int_0^\ell \cos[\beta_c(\ell-\xi)]d\xi = \frac{\sin \beta_c \ell}{\beta_c}\underline{E}_c^e \\ \underline{Z}\underline{W}_c(\ell) &= -j\underline{E}_c^e \int_0^\ell \sin[\beta_c(\ell-\xi)]d\xi \\ &= -\frac{j(1-\cos\beta_c\ell)}{\beta_c}\underline{E}_c^e \end{aligned}\right\} \quad (51)$$

$$\underline{K}_c(\ell) = -j\left[\frac{(1-\cos\beta_c\ell)\underline{I} - (jk^o\sin\beta_c\ell)\underline{P}}{\beta_c}\right]\underline{E}_c^e \quad (52)$$

$$\underline{S}_c = (k^i + k^o)\underline{P}\cos\beta_c\ell + j(\underline{I} + k^o k^i \underline{P}^2)\sin\beta_c\ell \quad (53)$$

Then,

$$\underline{Y}_c^i = \underline{S}_c^{-1}\underline{K}_c(\ell)$$

$$= \frac{1}{j\beta_c}[(k^i + k^o)\underline{P}\cos\beta_c\ell + j(\underline{I} + k^o k^i \underline{P}^2)\sin\beta_c\ell]^{-1}[(1-\cos\beta_c\ell)\underline{I} - jk^o\underline{P}\sin\beta_c\ell]\underline{E}_c^e$$

For small ℓ this is approximately

$$\underline{Y}_c^i = \frac{1}{j\beta_c}[(k^i + k^o)\underline{P} + j(\underline{I} + k^o k^i \underline{P}^2)\beta_c\ell]^{-1}[(\beta_c^2\ell^2/2)\underline{I} - jk^o\beta_c\ell\underline{P}]\underline{E}_c^e$$

Now, keeping ℓ fixed and small, but different from zero, let $\underline{P} \to \infty$ such that

$$Y_c^i \to \frac{1}{j\beta_c}[jk^o k^i \beta_c \ell \underline{P}^2]^{-1}[-jk^o\beta_c\ell\underline{P}]\underline{E}_c^e$$

$$= -\frac{\underline{P}^{-1}\underline{E}_c^e}{jk^i\beta_c} \to 0 \text{ as } \underline{P} \to \infty$$

Consequently,

$$\underline{I}_c^i = -\underline{Y}_c^i \underline{V}_c^i = -\underline{Y}\underline{P}_c^i \underline{V}_c^i$$

$$= -k^i \underline{Y}\underline{P} \underline{V}_c^i$$

$$= -k^i \underline{Y}\underline{P} \left[-\frac{\underline{P}^{-1} \underline{E}_c^e}{jk^i \beta_c} \right]$$

$$= \frac{\underline{Y}\underline{E}_c^e}{j\beta_c}$$

$$= -\frac{\omega I_g}{2\pi a \beta_c} \underline{Y}\underline{L}_c^e \qquad (54)$$

$$= -\frac{v_c I_g}{2\pi a} \underline{Y}\underline{L}_c^e \qquad (54a)$$

and, thus,

$$\underline{L}_c^e = -\frac{2\pi a \beta_c}{\omega I_g} \underline{Z}\underline{I}_c^i = -\frac{2\pi a}{v_c I_g} \underline{Z}\underline{I}_c^i \qquad (55)$$

where v_c is the velocity of propagation in the cable.

The foregoing analysis suggests a procedure for measuring the column vector L_c^e alone.

It requires a little extra care to show that $\underline{I}_c^o \to \underline{I}_c^i$ for small ℓ, as $\underline{P} \to \infty$ (see app B).

2.4.4 Open-Circuit Terminations: Solutions for Capacitive-Coupling Parameters

The appropriate schematic is shown in figure 6. We start with the assumption that $\ell << \lambda_c$, so that we can take

$$\left.\begin{aligned} \overline{H}_\phi &\equiv 0 \\ \overline{E}_r &= \text{constant} = -\frac{V_g}{a\ell n(b/a)} \quad \text{(fig. 3)} \\ &= -\frac{\eta_0 Y_{0s} V_g}{2\pi a} = -\frac{C_s V_g}{2\pi a \varepsilon_0} \end{aligned}\right\} \qquad (56)$$

where C_s is the capacitance per meter of the outer coax.

Then, from eq 32,

$$\left.\begin{aligned} \underline{E}_c^e &\equiv 0 \\ \underline{H}_c^e &= -\frac{j\omega C_s V_g}{2\pi a \varepsilon_0} \underline{C}_c^e \end{aligned}\right\} \qquad (57)$$

Open-circuit terminations imply that $\underline{P}_c^i$, $\underline{P}_c^o \to 0$. Furthermore, we have

$$\underline{U}_c(\ell) = -\frac{j\underline{Z}\underline{H}_c^e}{\beta_c} (1 - \cos \beta_c \ell) \qquad (58)$$

$$\underline{ZW}_c(\ell) = \underline{ZH}_c^e \frac{\sin \beta_c \ell}{\beta_c} \tag{59}$$

$$\underline{K}_c(\ell) = \underline{ZH}_c^e \frac{\sin \beta_c \ell}{\beta_c} \underline{I} + j\underline{P}_c^o \frac{1 - \cos \beta_c \ell}{\beta_c}$$

for $\ell << \lambda_c$

$$\simeq \underline{ZH}_c^e [\ell \underline{I} + j\underline{P}_c^o (\beta_c \ell^2/2)] \tag{60}$$

$$S_c \simeq (\underline{P}_c^i + \underline{P}_c^o)(-\beta_c \ell^2/2) + j(\underline{I} + \underline{P}_c^o \underline{P}_c^i)\beta_c \ell$$

For fixed ℓ, and $\underline{P}_c^i$, $\underline{P}_c^o \to 0$,

$$\underline{U}_c(\ell) \to 0$$

$$\underline{K}_c(\ell) \to \underline{ZH}_c^e \ell$$

$$\underline{S}_c \to j\beta_c \ell \underline{I}$$

Therefore,

$$\underline{V}_c^i \to \underline{V}_c^o \to (j\beta_c \ell \underline{I})^{-1} (\underline{ZH}_c^e \ell) = \frac{\underline{ZH}_c^e}{j\beta_c} \tag{61a}$$

$$= - \frac{\omega C_s V_g}{2\pi a \epsilon_0 \beta_c} \underline{ZC}_c^e = - \frac{\omega \eta_0 Y_{0s} V_g}{2\pi a \beta_c} \underline{ZC}_c^e \tag{61b}$$

which leads to

$$\underline{C}_c^e = - \frac{2\pi a \epsilon_0 \beta_c}{\omega C_s V_g} \underline{YV}_c^i = - \frac{2\pi a \beta_c}{\omega \eta_0 Y_{0s} V_g} \underline{YV}_c^i = - \frac{2\pi a}{v_c \eta_0 Y_{0s} V_g} \underline{YV}_c^i \tag{62}$$

Assuming media permeabilities to be equal, we can write

$$v_c \eta_0 = (\mu_0 \epsilon_c)^{-1/2} (\mu_0/\epsilon_0)^{1/2} = (\epsilon_c \epsilon_0)^{-1/2}$$

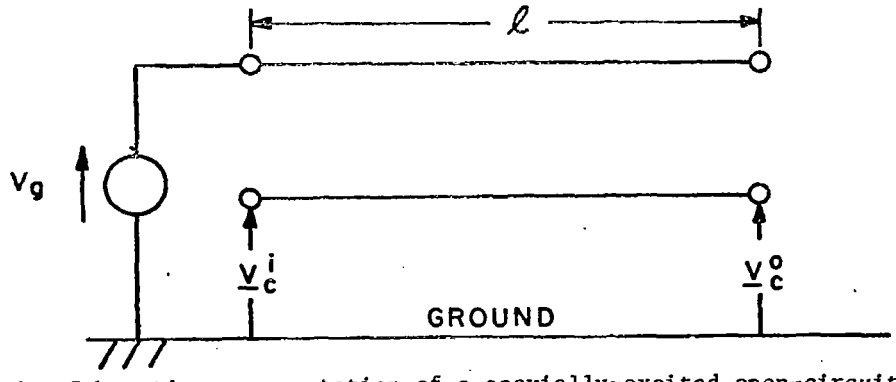

Figure 6. Schematic representation of a coaxially-excited open-circuited cable.

so that, finally,

$$\underline{C}_c^e = - \frac{2\pi a \sqrt{\varepsilon_c \varepsilon_0}}{Y_{0s} V_g} \underline{Y} \underline{V}_c^i \qquad (63)$$

Eq 63 and figure 6 suggests a procedure for measuring the column vector $\underline{C}_c^e$ alone.

2.4.5 Discussion

This analysis presumes that the external field coupling parameters are of two kinds--electric and magnetic--and that both must be known before the cable response can be determined. The analysis also indicates that the relative importance of the two kinds of parameters depends on the nature of the cable terminations and on the relative magnitudes of the coupling parameters themselves. As to the latter, adequate evidence exists to suggest that, under line-match conditions, their effects may be expected to be of the same order of magnitude (see sec. 2.6, fig. 10).

In view of these facts, it is somewhat mystifying to discover that the literature (ref 19 and 20, among others) is pre-occupied with the effect of the sheath surface current, which is a direct measure of the average sheath tangential magnetic intensity, and ignores the applied potential difference, which is related to the sheath normal electric intensity. For the case in which the cable under study is a simple coaxial cable (N = 1), methods of experimental implementation have enjoyed a considerable number of closely related variations (ref 2, 8-12).

2.5 Review of Published Procedures for Coupling Measurement: Relation to Present Analysis

All of the methods to be discussed use the basic coaxially-coupled arrangement of section 2.4, with N = 1. All of the methods define shielding effectiveness or transfer impedance in terms of a single coupling parameter, whereas the foregoing development suggests that two are required to determine the cable terminal response.

Table I compares the definitions and experimental arrangements of five sets of experimenters. Among these, three basically different results are obtained. The method of Knowles and Olson (ref 12) yields a result which essentially depends on the sum of the inductive-reactance and capacitive-susceptance coupling through the braid. On the other hand, the method of Zorzy and Muehlberger (ref 2) and one of Krügel's (ref 9) depends on the difference of these quantities. The third basic method--that of Vance and Chang (ref 8), Miller and Toulios (ref 11), and the other of Krügel's arrangements--measure the inductive coupling effect alone. Combining the first two of these (i.e., classes I and III of the table) could yield the complete information required, as suggested by the analysis of section 2.4.2. Alternatively, the method of section 2.4.5, combined with class II of table I, could yield an equivalent result.

---

[19] Latham, R.W., "An Approach to Certain Cable Shielding Calculations," Note 90, Air Force Weapons Lab EMP Interaction Notes, January 1972, Kirtland AFB, New Mexico.

[20] Vance, E.F., "Comparison of Electric and Magnetic Coupling through Braided-Wire Shields," Technical Memorandum No. 18, AFWL Contract F29601-69-C-0127, February 1972, Kirtland AFB, New Mexico.

Ignoring the capacitance parameter can only be justified if its effect on cable terminations can be shown to be insignificant compared to that of the inductive parameter. These effects depend not only on the relative magnitudes of the coupling admittances, but on the nature of shield ground, the nature of cable terminations, the length of the cable, and the orientation and polarization of the external impressed fields. All of these factors, with the exception of the relative magnitudes of the coupling parameters, have been discussed to some extent in the preceding sections. The next section briefly reviews the work of Vance and Chang (ref 8) and of Vance (ref 20), covering this final aspect of the problem.

2.6 Coupling of Coaxial Guides through Small Apertures

We will use the concepts and results set forth in the work of Marcuvitz (ref 7) and Vance and Chang (ref 8). For higher frequencies, where diffusion directly through the shield conductor is negligible, coupling is conceived as occurring by leakage of the exterior fields through rhomboidal-shaped apertures formed by openings between crisscrossed wires of the braid carriers (ref 8). In view of the difficulties involved in analytically assessing the effects of apertures of this shape, the fact that solutions for elliptical apertures are available (ref 6, 7) and the results of some experiments suggesting that the gross coupling effects are not highly sensitive to details of aperture shape (ref 21), Vance and Chang elect to replace the rhomboidal shape with an ellipse whose axes are of the same length as the diagonals of the rhomboid as displayed in figure 8. If α is the weave angle of the braid carriers with the axis of the cable, and ℓ_h and w_h are the semi-major and semi-minor axes of the ellipse, respectively, then the eccentricity of the ellipse is

$$e = \left[1 - \left(\frac{w_h}{\ell_h}\right)^2\right]^{1/2} = (1 - \tan^2 \alpha)^{1/2};\ 0 \le \alpha \le \pi/4 \qquad = (1 - \cot^2 \alpha)^{1/2};\ \pi/4 \le \alpha \le \pi/2 \tag{64}$$

Thus the braided shield is replaced by a solid conductor perforated by a large number of elliptical holes which are assumed so small compared to their spacings that their effects do not interact. Vance and Chang calculate the number of these holes per meter of shield (υ_h) to be

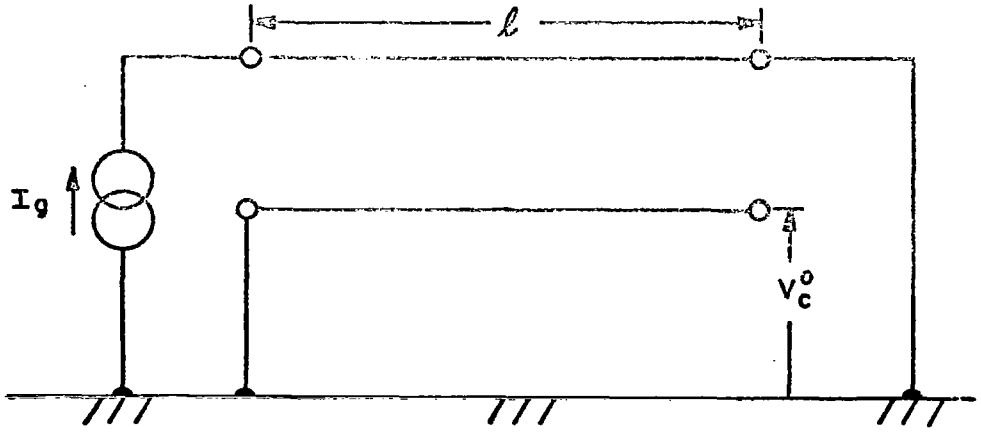

Figure 7. Schematic diagram for definition and measurement of shielding effectiveness.

TABLE I. VARIOUS DEFINITIONS AND METHODS OF MEASUREMENT: SHIELDING EFFECTIVENESS AND TRANSFER IMPEDANCE

Class	Author(s)	Figure 3 Terminations				Schematic	Shielding Effectiveness or Transfer Impedance Definition
		1	2	3	4		
I	Knowles & Olson[12]	source	match termination	match detector	match termination	Figure 4 (N = 1)	S.E. = 20 $\log\left\|\frac{I_g}{I_c}\right\|$ ⓐ
II	Vance & Chang[8] Miller & Toulios[11]	source	short-circuit	short-circuit	open-circuit detector	Figure 7	$Z_T = -\frac{V_c^o}{I_g^\ell}$ ⓑ
III	Zorzy & Muehlberger[2] Krügel[9]	match termination	match detector	source	match termination	Figure 4 (N = 1), except roles of inner and outer lines interchanged	$A = \left\|\frac{I_g^2 Z_{0c}}{(I_s^o)^2 Z_{0s}}\right\|$ ⓒ
IV	Krügel[9]	short-circuit	open-circuit detector	source	short-circuit	Figure 7, except roles of inner and outer lines interchanged	$Z_T = \frac{V_s^o}{I_g^\ell}$ ⓓ

ⓐ S.E. = shielding effectiveness
ⓑ Z_T = transfer impedance
ⓒ A = leakage power ratio; Z_{0c} = characteristic impedance of cable
ⓓ V_s^o = outer line output voltage

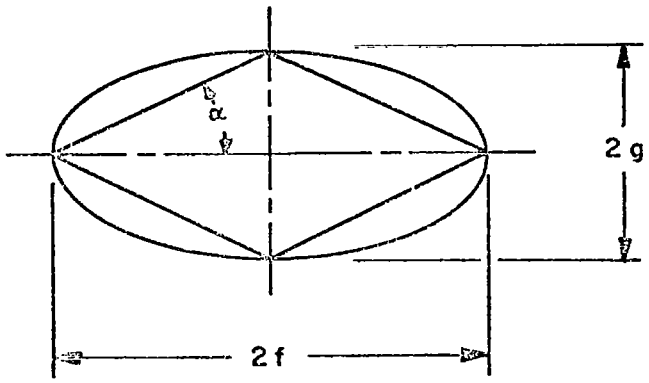

Figure 8. Rhomboid with diagonals 2f and 2g replaced by ellipse with semi-axes f and g, respectively.

$$\upsilon_h = \frac{4\pi a \sin\alpha \cos\alpha}{d^2} F^2 \qquad (65)$$

where a is the radius of the perforated shield, d is the diameter of an individual conductor in the braid carrier. F is the relative coverage of one carrier of the braid

[21] Cohn, S.B., "Determination of Aperture Parameters by Electrolytic-Tank Measurements," Proc. IRE, Vol. 39, No. 11, November 1951, pp. 1416-1421.

Formulas	Comments
$S.E. = 20 \log \frac{4\pi a}{\omega(L_c^e Y_{0c} - C_c^e \eta_0)\ell}$; $\ell \ll \lambda_c$	1. Measures sum of magnetic and electric coupling effects, since $L_c^e \geq 0$, while $C_c^e \leq 0$. 2. Shielding effectiveness formula follows from eq 44a & 46.
$Z_T = j\omega \frac{L_c^e}{2\pi a}$; $\ell \ll \lambda_c$	1. Measures L_c^e alone. 2. Formula for transfer impedance derived in appendix C.
$A = \left\lvert \frac{4\pi a(\beta_s - \beta_c)}{\omega(L_c^e Y_{0s} + C_c^e \eta_c)[\exp(-j\beta_s \ell) - \exp(-j\beta_c \ell)]} \right\rvert^2 \frac{Z_{0c}}{Z_{0s}}$; ℓ not necessarily small	1. Measures difference of magnetic and electric coupling effects, since $L_c^e \geq 0$, while $C_c^e \leq 0$. 2. Leakage power ratio follows from eq 44b & 46, with appropriate permuting of subscripts.
Same as II with appropriate permuting of symbols.	Same as II with appropriate permuting of subscripts.

$$F = pnd \csc \alpha \tag{66}$$

where n is the number of wires in each braid carrier, and p (the picks) is the number of carrier crossings per meter of cable. If C is the total number of carriers, or belts of wires,

$$p = \frac{C}{4\pi a} \tan \alpha \tag{67}$$

Marcuvitz (ref 7) shows an equivalent circuit for coupling between coaxial guides with air dielectric, when coupling is through a small elliptical aperture in their common, zero-thickness wall. For our purposes, this can be represented by figure 9. We have, if the dielectric is air throughout,

$$\left.\begin{aligned} \omega L_m &= \frac{\eta_0 M}{2\pi\lambda_0 a^2} \\ \omega C_m &= \frac{P\eta_0 Y_{0s} Y_{0c}}{2\pi\lambda_0 a^2} \end{aligned}\right\} \tag{68}$$

where Y_{0s} and Y_{0c} are the characteristic admittances of outer and inner coaxial lines respectively, and (ref 6-8)

$$\left.\begin{aligned} M &= \frac{\pi \ell_h^3}{24} \frac{e^2(1 - e^2)}{E(e) - (1 - e^2)K(e)} \quad ; \quad 0 \leq \alpha \leq \pi/4 \\ &= \frac{\pi \ell_h^3}{24} \frac{e^2}{K(e) - E(e)} \quad ; \quad \pi/4 \leq \alpha \leq \pi/2 \\ P &= \frac{\pi \ell_h^3}{24} \frac{1 - e^2}{E(e)} \end{aligned}\right\} \tag{69}$$

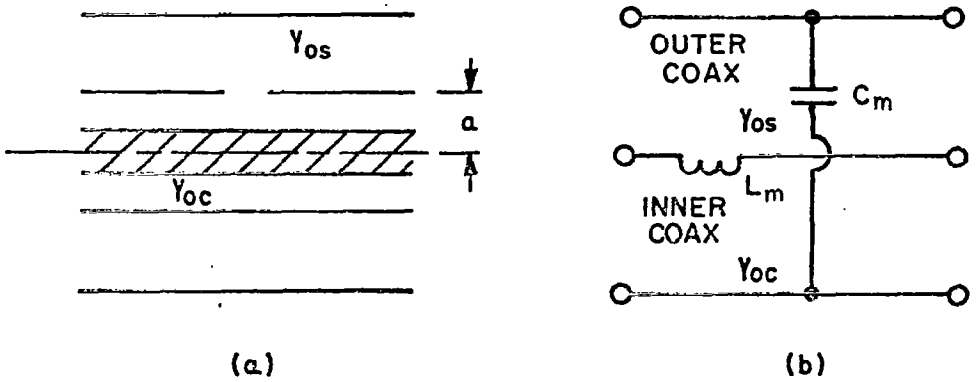

Figure 9. Coaxial guides coupled through a small hole in their common wall; (a) longitudinal-section; (b) equivalent circuit.

where K(e) and E(e) are the complete elliptic integrals of the first and second kinds, respectively

$$\left.\begin{aligned} K(e) &= \int_0^{\frac{\pi}{2}} (1 - e^2\sin^2\phi)^{-1/2}d\phi \\ E(e) &= \int_0^{\frac{\pi}{2}} (1 - e^2\sin^2\phi)^{1/2}d\phi \end{aligned}\right\} \quad (70)$$

When the dielectric of the outer coax is air and that of the inner coax has a relative dielectric constant ε_r different from one, the coupling inductance L_m is independent of ε_r, and the result calculated from the first of eq 68 remains correct.

With regard to C_m, however, we are not yet in a position to correctly estimate the effect of increasing the dielectric constant of the inner coax alone. If the dielectric constant were changed throughout by ε_r, then C_m should change by the same factor. In the right member of the second of eq 68, both Y_{0s} and Y_{0c} would change by $\sqrt{\varepsilon_r}$, so that the second of eq 68 yields the correct value of C_m for any uniform value of ε_r in both lines. When only the inner coax has a relative dielectric constant ε_r different from one, the right member of the second of eq 68 is increased by only $\sqrt{\varepsilon_r}$. On the other hand, the normal flux through the aperture will probably increase only slightly, and part of the increase is likely to return to the inner surface of the common wall. Altogether, we can only guess that the formula for C_m needs a correction factor $k(\varepsilon_r)$, where k is expected to be in the vicinity of $1/\sqrt{\varepsilon_r}$.

If we have υ_h holes per meter of line, with axial hole distance small compared to a wavelength, then we can treat $\upsilon_h L_m$ and $\upsilon_h C_m$ as continuous coupling parameters for the line. For the cable (inner coax), we have

$$\left.\begin{aligned} \frac{dV_c}{dx} + j\omega L_c I_c &= -j\omega\upsilon_h L_m I_s = E_c^e(x) \\ \frac{dI_c}{dx} + j\omega C_c V_c &= j\omega\upsilon_h C_m V_s = H_c^e(x) \end{aligned}\right\} \quad (71)$$

where L_c and C_c are the inductance and capacitance per meter of inner coax, respectively. By eq 32,

$$\left.\begin{aligned} E_c^e(x) &= j\omega L_c^e \overline{H_\phi(x)} = -j\omega L_c^e \frac{I_s}{2\pi a} \\ H_c^e(x) &= j\omega C_c^e \overline{E_r(x)} = -j\omega C_c^e \frac{C_s V_s}{2\pi\varepsilon_0 a} \end{aligned}\right\} \quad (72)$$

where C_s is the capacitance per meter of the outer coax. Comparing eq 71 and 72, we get

$$\left.\begin{aligned} L_c^e &= 2\pi a \upsilon_h L_m \\ C_c^e &= -\frac{2\pi a \upsilon_h C_m}{\eta_0 Y_{0s}} \end{aligned}\right\} \quad (73)$$

Then, substitution from eq 68 and the use of other standard substitution yields

$$\left.\begin{aligned} L_c^e &= \frac{\upsilon_h \mu_0 M}{2\pi a} \\ C_c^e &= -k(\varepsilon_r)\frac{\upsilon_h P Y_{0c}}{2\pi a v_0} \end{aligned}\right\} \quad (74)$$

where v_0 is the free-space propagation velocity (3×10^8 m/s), and the factor $k(\varepsilon_r)$ has been added to the second equation to indicate the vagueness in our information regarding this parameter when the coupled lines have different dielectrics. Our best guess is that k is in the vicinity of $1/\sqrt{\varepsilon_r}$.

Vance (ref 20) has calculated $\upsilon_h L_m$ for various braid parameter values in order to compare his theory with measurements made by Krügel. Agreement was generally within a factor of two: a very satisfactory result considering the approximate nature of the physical model, and considering the possibility that some of the experimental data were derived from Krügel's Class III (table I) measurements.

It is interesting to compare the relative effects of external electric and magnetic intensities under some form of standard conditions. Perhaps a reasonable set of such conditions is that leading to eq 44: i.e., coupling through a braid acting as the common wall of a matched triaxial system (N = 1). In that case, eq 44 contains the composite coupling factors

$$L_c^e \pm \eta_0 Z_{0c} C_c^e$$

and the relative effects of the two types of coupling may be measured by the relative values of the magnitudes of the two coupling terms; that is,

$$R = \left| \frac{L_c^e}{\eta_0 Z_{0c} C_c^e} \right| \quad (75)$$

Using eq 73 (which assumes equal dielectric properties in both lines) in eq 75,

$$R = \frac{L_m Y_{0s} Y_{0c}}{C_m} \quad (76)$$

Then, eq 68 in eq 76 yields

$$R = \frac{\omega L_m}{\omega C_m} Y_{0s} Y_{0c} = \frac{M}{P} \tag{77}$$

where M and P are given by eq 69.

Eq 77 has been computed and plotted by Vance (ref 20). Figure 10 of this report is essentially figure 3 given by Vance, modified for changes in notation. For typical weave angles in the region of 30° to 45°, the ratio runs from about 1.5 to about 2. At a weave angle of 30°, this implies a ratio of 5:1 in V_i^i and V_c^o (eq 44), or about 14 dB. Thus, in attributing the whole coupling effect to a surface transfer impedance, the method of Knowles and Olson (ref 12 and table I) under the conditions stated above, exaggerate the role of the inductive parameter by 5/3, or 4.4 dB, while that of Zorzy and Muehlberger (ref 2 and table I) understates it by a factor of 1/3, or 9.6 dB. The ratio of outputs at the two matched terminals is plotted as a function of weave angle in figure 11.

Note that in the limiting case when $\alpha = 0$, we have $R = 1$ and the ratio of outputs is infinite ($V_c^o = 0$). In fact, we have the condition for perfect directivity, as in the case of the TEM distributed coupler (ref 18, 22).

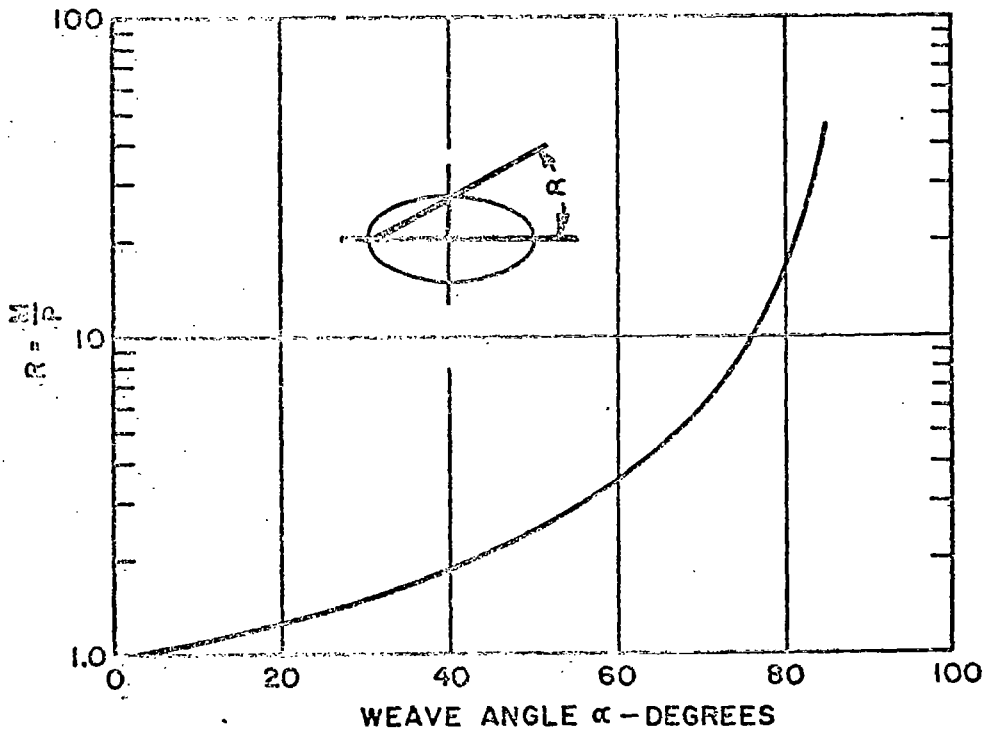

Figure 10. Ratio of magnetic to electric polarizability as a function of braid weave angle.

[22] Matthaei, G.L., Young, L., and Jones, E.M.T., Microwave Filters, Impedance-Matching Networks, and Coupling Structures, McGraw-Hill, New York, 1964.

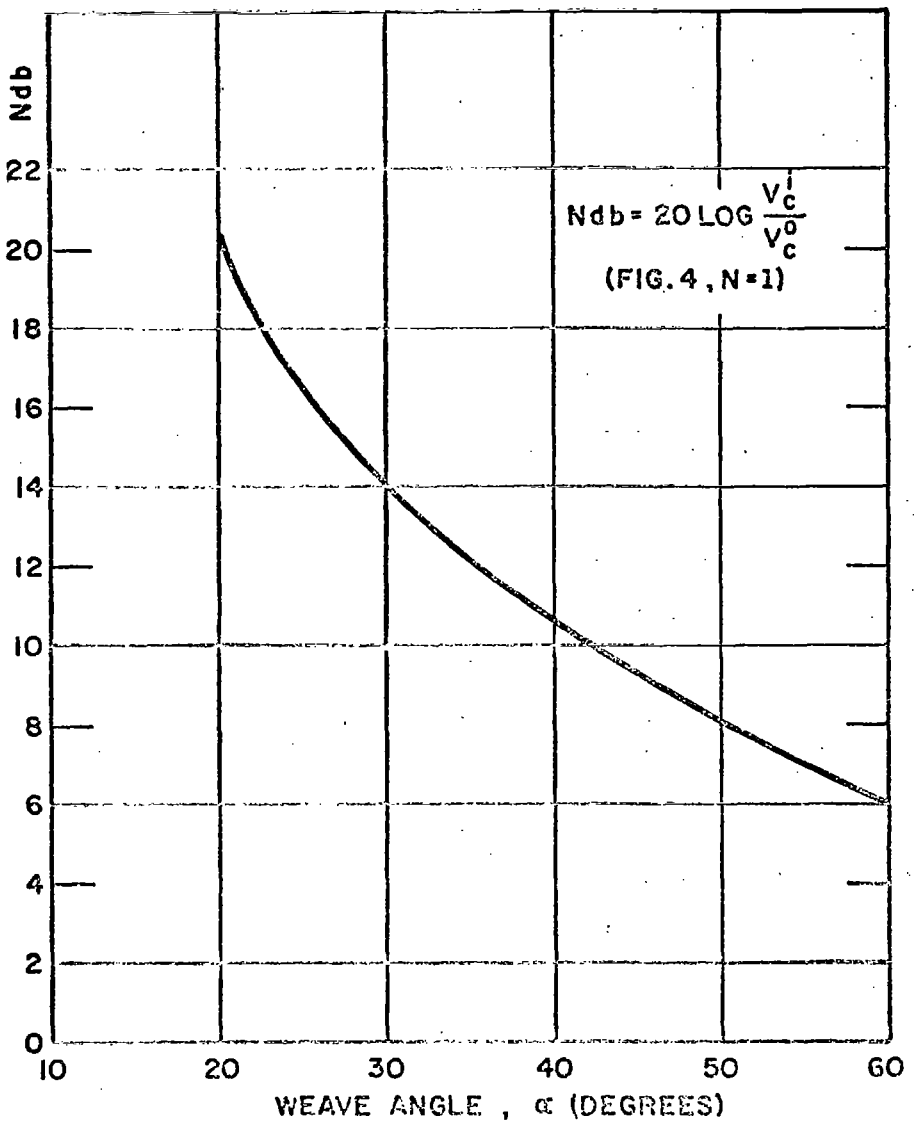

Figure 11. Ratio of outputs at matched terminals as a function of weave angle.

3. DISCUSSION OF RESULTS

This study has had two purposes: (1) to assess the relative importance of magnetic and electric coupling parameters of braided shields in determining the terminal response of braided cables to external electromagnetic fields, and (2) to investigate and exhibit any discrepancies between the coupling model postulated here and those on which various experimental determinations of shielding effectiveness have been based.

In the first instance, the study was specialized to two practical cases of interest: i.e., those in which the shield is grounded either at one or at both ends of the cable. Results were given for fairly general external field conditions and were also specialized to two situations of interest: (1) a horizontally polarized wave incident in the transverse plane of the cable, and (2) a vertically polarized wave travelling along the cable axis. In only one of these cases was the effect of the electric charge induced on the cable exterior clearly shown to be negligible: the case of transverse incidence on a cable grounded at both ends.

However, in the other cases, no effort has been made to determine the relative importance of surface current and surface charge in each instance, or the relative total strength of coupling to the terminations for the various examples chosen. Also, this whole study has been in the frequency domain; in the final analysis, transient time-domain information is required. In view of the limited data obtained so far, the results of this aspect of the study must be considered as only preliminary, even though they now appear adequate for further detailed analysis.

In the second instance, that of shielding-effectiveness measurements, it seems clear that the study has focused on a number of discrepancies, not only among the various methods of measurement, but between the measurements and the postulated model as well. Even if further analysis shows the electric coupling parameter to be unimportant in practical situations, the methods of Knowles and Olson (ref 12) and of Zorzy and Muehlberger (ref 2) appear to disagree with each other, and each disagrees with the model in assessing the value of the inductive parameter.

The study has also yielded results which show, at least formally, how the coupling parameters to each conductor of a multi-conductor cable may be determined.

Finally, we wish to suggest a small modification in the definition of series-transfer impedance and to join it with a companion definition of shunt-transfer susceptance, as expressed by the following equations:

$$\left.\begin{aligned} &\text{Series-transfer impedance:} \quad Z_T = \frac{E_c^e}{H_\phi} = \frac{2\pi a E_c^e}{I_s} = j\omega L_c^e \\ &\text{Shunt-transfer admittance:} \quad Y_T = \frac{H_c^e}{E_r} = \frac{2\pi a \varepsilon_o H_c^e}{q_s} = j\omega C_c^e \end{aligned}\right\} \qquad (78)$$

where q_s is the surface charge on the sheath exterior in coulombs/meter (C/m).

4. CONCLUSIONS

In general, the inner conductors of a braided-sheath cable subjected to an external electromagnetic field receive energy leaked through the sheath by both inductive-impedance and capacitive-susceptance transfer mechanisms. Formal results expressing the terminal responses in terms of the cable parameters and terminations, and the

orientation of the external fields, have been obtained in general, and also for certain special cases. However, the implications of these results have not been explored in detail. From a practical standpoint, the external coupling parameters are best determined by measurement, although an interesting approximate model suggested by others is available.

On the basis of results obtained in this study, we must conclude that measurements of shielding effectiveness made in the past have been largely incomplete. These measurements were either sufficient to determine only the inductance parameter, or they represented a composite result of inductive and capacitive coupling that was attributed to inductive coupling alone. In either case, such measurements are insufficient for characterizing a cable response to an external electromagnetic field.

5. LITERATURE CITED

1. Schelkunoff, S.A. and Odarenko, T.M., "Cross-Talk between Coaxial Lines," Bell System Technical Journal, Vol. 16, No. 2, April 1937, pp. 144-164.
2. Zorzy, J. and Muehlberger, R.F., "RF Leakage Characteristics of Popular Coaxial Cables and Connectors, 500 Mc to 7.5 Gc," Microwave Journal, Vol. 4, No. 11, November 1961, pp. 80-86.
3. Sidney Frankel & Associates, Menlo Park, California, "Penetration of a Travelling Surface Wave into a Coaxial Cable (First Interim Report)," Sandia Report SC-CR-67-2702, August 1967.
4. Bethe, H.A., "Theory of Diffraction by Small Holes," Physical Review, Second Series, Vol. 66, No. 7 and 8, October 1 and 15, 1944, pp. 163-182.
5. Kaden, H., Wirbelströme und Schirmung in der Nachrichtentechnik, Springer-Verlag, Berlin, 1959.
6. Montgomery, C.G., Dicke, R.H., and Purcell, E.M., Principles of Microwave Circuits, MIT Radiation Laboratory Series, Vol. 8, McGraw-Hill, New York, 1948.
7. Marcuvitz, N., Waveguide Handbook, MIT Radiation Laboratory Series, Vol. 10, McGraw-Hill, New York, 1948.
8. Vance, E.F. and Chang, H., "Shielding Effectiveness of Braided-Wire Shields," Technical Memorandum No. 16, AFWL Contract F29601-69-C-0127, November 1971.
9. Krügel, L., "Shielding Effectiveness of Outer Conductors of Flexible Coaxial Cable," (Abschirmwirkung von Aussenleitern Flexibler Koaxialkable), Telefunken-Zeitung, Vol. 29, December 1936, pp. 256-266.
10. Osborn, D.C. and Petschek, A.G., "Computer Analysis of Coupling in Braid-Shielded Cable," Systems, Science, and Software Report 3SR-276-1, 8 June 1970, La Jolla, California.
11. Miller, D.A. and Toulios, P.P., "Penetration of Coaxial Cables by Transient Fields," IEEE EMC Symposium Record, 1968, pp. 414-423.
12. Knowles, E.D. and Olson, L.W., "Braided Cable Shielding Effectiveness Study," Boeing Company REV LTR, Code Ident. No. 81205, Number T2-3886-1, October 9, 1970.

13. Harrison, C.W., "Bounds on the Load Current of Exposed One- and Two-Conductor Transmission Lines Electromagnetically Coupled to a Rocket," IEEE, Trans. in Electromagnetic Compatability, Vol. EMC-14, No. 1, pp. 4-9, February 1972.

14. Sidney Frankel & Associates, Menlo Park, California, Interim Report, "Response of a Multiconductor Transmission Line to Excitation by an Arbitrary Monochromatic Impressed Field along the Line," Sandia Report SC-CR-71 5076, April 1971.

15. Frankel, S., "TEM Response of a Multiwire Transmission Line (Cable) to an Externally-Impressed Electromagnetic Field: Recipe for Analysis," Harry Diamond Laboratories, Washington, D.C.

16. Frankel, S., "Externally-Excited Transmission Line: Definition of Procedures for Determining Coupling Parameters," Harry Diamond Laboratories HDL-TM-72-11, April 1972.

17. Frankel, S., "Field Coupling Parameters for a Single Round Wire Close to a Ground Plane or Two Large Round Wires in Free Space," Harry Diamond Laboratories HDL-TM-72-14, April 1972.

18. Uchida, Hidenari, Fundamentals of Coupled Lines and Multi-Wire Antennas, Sasaki Publishing Co., Sendai, Japan, 1967.

19. Latham, R.W., "An Approach to Certain Cable Shielding Calculations," Note 90, Air Force Weapons Lab EMP Interaction Notes, January 1972, Kirtland AFB, New Mexico.

20. Vance, E.F., "Comparison of Electric and Magnetic Coupling through Braided-Wire Shields," Technical Memorandum No. 18, AFWL Contract F29601-69-C-0127, February 1972, Kirtland AFB, New Mexico.

21. Cohn, S.B., "Determination of Aperture Parameters by Electrolytic-Tank Measurements," Proc. IRE, Vol. 39, No. 11, November 1951, pp. 1416-1421.

22. Matthaei, G.L., Young, L., and Jones, E.M.T., Microwave Filters, Impedance-Matching Networks, and Coupling Structures, McGraw-Hill, New York, 1964.

SYMBOL INDEX

Symbol	Defined or Mentioned Initially on Page
a	8
C	31
C_c	33
$\underline{C}^e_c$, $C^e_{c,i}$	19
C_m	32
C_s	33
C^e_s	11
d	31
e	30
$E(e)$	32
$E_r(x)$	12
$E^e_y(x)$, E^e_z	9
$\underline{E}^e_c(x)$	18
$E^e_s(x)$	11
F	31
$G(\rho)$	13
$H^e_z(x)$	9
$H_\phi(x)$	12
$\underline{H}^e_c(x)$	12
$H^e_s(x)$	11
h	10
$\underline{I}^i_c$, $I^i_{c,i}$	18
$\underline{I}^o_c$, $I^o_{c,i}$	18
I_g	22
$I_s(x)$	10
I^i_s, I^o_s	10
$\underline{I}$	18
$K(e)$	32
$\underline{K}_c(\ell)$	18
$\underline{K}_s(\ell)$	10
$k(\varepsilon_r)$	32
k^i, k^o	24
L_c	33
$\underline{L}^e_c$, $L^e_{c,i}$	19
L_m	33
L^e_s	11
ℓ	8
ℓ_h	30
M	31
N	8
n	31
P	44
$\underline{P}$	18
$\underline{p}^i_c$, $\underline{p}^o_c$	10
$\underline{p}^i_s$, $\underline{p}^o_s$	18
p	31
q_s	36

Symbol	Defined or Mentioned Initially on Page
R	33
$\underline{S}_c$	18
S_s	10
$\underline{T}$	44
TEM	9
$\underline{U}_c(\ell)$	18
$U_s(\ell)$	10
$\underline{V}_c^i$, $V_{c,i}^i$	18
$\underline{V}_c^o$, $V_{c,i}^o$	18
V_g	22
$V_s(x)$	10
V_s^i, V_s^o	10
v_c	26
v_o	12
$\underline{W}_c(\ell)$	18
$W_s(x)$	10
w_h	30
$\underline{Y}$, Y_{ij}	18
$\underline{Y}_c^i$, $Y_{c,ij}^i$	18
$\underline{Y}_c^o$, $Y_{c,ij}^o$	18
Y_s^i, Y_s^o	10
Y_T	36
Y_{0c}	31
Y_{0s}	31
$\underline{Z}$, Z_{ij}	18
Z_T	36

Symbol	Defined or Mentioned Initially on Page
Z_{0s}	10
α	34
α_s	13
β_c	18
β_e	12
β_s	10
γ_s	13
ϵ_o	13
ϵ_r	32
η_o	13
λ_c	22
λ_o	22
μ_o	11
ν	13
υ_h	30
ρ	11
$\phi_{c,\ell}$	23
$\phi_{s,\ell}$	23
$\phi_{s,x}$	23
$\psi_{c,\ell}$	23
$\psi_{s,\ell}$	23
$\psi_{s,x}$	24
ω	31

Appendix A

Cable Sheath Grounded at One End: Derivation of Eq 10

Assume the sheath grounded at the input end, open-circuited at the output. Then,

$$P_s^I \to \infty \; ; \; P_s^O \to 0$$

The first of eq 1 yields

$$S_s \to P_s^I \cos \beta_s \ell$$

From the second of eq 1,

$$K_s(\ell) = Z_{0s} W_s(\ell)$$

We also have the well-known formula

$$Z_{0s} = \frac{1}{Y_{0s}} = 60 \cosh^{-1} \rho = \frac{1}{2\pi} \sqrt{\frac{\mu_0}{\epsilon_0}} \cosh^{-1} \rho$$

$$= \frac{\eta_0}{2\pi} \cosh^{-1} \rho = \frac{1}{v_0 C_s} \qquad \text{(A-1)}$$

where C_s is the capacitance of the sheath with respect to ground, per meter of cable. Thus eq 3 becomes

$$I_s(x) \to -Y_{0s}(P_s^i \cos \beta_s x)\left(\frac{Z_{0s} W_s(\ell)}{P_s^i \cos \beta_s \ell}\right) + W_s(x)$$

i.e.,

$$I_s(x) = W_s(x) - W_s(\ell)\left(\frac{\cos \beta_s x}{\cos \beta_s \ell}\right) \qquad \text{(A-2)}$$

Define

$H_\phi(x)$ = tangential magnetic intensity at outer surface of sheath (A/m)
$E_r(x)$ = normal electric intensity at outer surface of sheath (V/m)

By Ampere's theorem, the average value of the magnetic intensity around the conductor periphery is

$$\overline{H_\phi(x)} = \frac{1}{2\pi}\int_0^{2\pi} H_\phi(x) d\phi = \frac{I_s(x)}{2\pi a} \qquad \text{(A-3)}$$

By Gauss' theorem, the average value of the electric intensity is

$$\overline{E_r(x)} = \frac{1}{2\pi}\int_0^{2\pi} E_r(x) d\phi = \frac{q_s(x)}{2\pi a \epsilon_0}$$

where $q_s(x)$ is the total charge induced on the sheath per meter of line, and ϵ_0 is the dielectric permittivity of the air in farads per meter (F/m):

$$\epsilon_0 = \frac{10^{-9}}{36\pi}$$

The law of current continuity requires

$$\frac{dI_s}{dx} + j\omega q_s = 0$$

whence

$$\overline{E_r(x)} = -\frac{1}{j2\pi a\epsilon_0\omega}\frac{dI_s}{dx} \tag{A-4}$$

From eq A-2 the value of the current derivative is

$$\frac{dI_s}{dx} = \frac{dW_s}{dx} + \beta_s W_s(\ell)\frac{\sin\beta_s x}{\cos\beta_s \ell} \tag{A-5}$$

Therefore, by eq A-3 and A-4,

$$\left.\begin{aligned}\overline{H_\phi(x)} &= \frac{\sec\beta_s\ell}{2\pi a}\left[W_s(x)\cos\beta_s\ell - W_s(\ell)\cos\beta_s x\right]\\ \overline{E_r(x)} &= -\frac{\sec\beta_s\ell}{j2\pi a\epsilon_0\omega}\left[\frac{dW_s}{dx}\cos\beta_s\ell + \beta_s W_s(\ell)\sin\beta_s x\right]\\ 0 &\le x \le \ell\end{aligned}\right\} \tag{A-6}$$

$W_s(x)$ is given by the second of eq 8. Differentiate that equation to obtain

$$\frac{dW_s}{dx} = H_s^e(0)\frac{d\phi_{s,x}}{dx} - jY_{0s}E_s^e(0)\frac{d\psi_{s,x}}{dx} \tag{A-7}$$

The indicated derivatives are evaluated from eq 9:

$$\left.\begin{aligned}\frac{d\phi_{s,x}}{dx} &= \frac{-j\beta_e\beta_s\sin\beta_s x + \beta_s^2\cos\beta_s x - \beta_e^2\exp(-j\beta_e x)}{\beta_s^2 - \beta_e^2}\\ \frac{d\psi_{s,x}}{dx} &= \frac{j\beta_e\beta_s\cos\beta_s x + \beta_s^2\sin\beta_s x - j\beta_s\beta_e\exp(-j\beta_e x)}{\beta_s^2 - \beta_e^2}\\ \beta_s &\neq \beta_e\end{aligned}\right\} \tag{A-8}$$

Making the appropriate substitutions and reducing,

$$\left.\begin{aligned}\overline{H_\phi(x)} &= \frac{\sec\beta_s\ell}{2\pi a(\beta_s^2 - \beta_e^2)}\left\{[\beta_s H_s^e(0) + \beta_e Y_{0s}E_s^e(0)]\sin[\beta_s(x-\ell)]\right.\\ &\quad\left. - j[\beta_e H_s^e(0) + \beta_s Y_{0s}E_s^e(0)][\exp(-j\beta_e x)\cos\beta_s\ell - \exp(-j\beta_e\ell)\cos\beta_s x]\right\}\\ \overline{E_r(x)} &= -\frac{\sec\beta_s\ell}{j2\pi a\epsilon_0\omega(\beta_s^2 - \beta_e^2)}\left\{\beta_s[\beta_s H_s^e(0) + \beta_e Y_{0s}E_s^e(0)]\cos[\beta_s(x-\ell)]\right.\\ &\quad\left. - [\beta_e H_s^e(0) + \beta_s Y_{0s}E_s^e(0)][\beta_e\exp(-j\beta_e x)\cos\beta_s\ell + j\beta_s\exp(-j\beta_e\ell)\sin\beta_s x]\right\}\\ 0 &\le x \le \ell;\ \beta_s \neq \beta_e\end{aligned}\right\} \tag{A-9}$$

In eq A-9, write

$$\nu = \frac{\beta_e}{\beta_s};\ 0 \le \nu < 1 \tag{A-10}$$

Also use eq 4,5 and A-1 to get

$$\left.\begin{aligned} \frac{H_s^e(0)}{2\pi a\beta_s} &= -j\,\frac{\sqrt{\rho^2-1}}{\cosh^{-1}\rho}\,\frac{E_y^e(0)}{\eta_0} \\ \frac{Y_{0s}E_s^e(0)}{2\pi a\beta_s} &= j\,\frac{\sqrt{\rho^2-1}}{\cosh^{-1}\rho}\,H_z^e(0) \end{aligned}\right\} \qquad \text{(A-11)}$$

and

$$\frac{H_s^e(0)}{Y_{0s}E_s^e(0)} = -\frac{E_y^e(0)}{\eta_0 H_z^e(0)} \qquad \text{(A-12)}$$

Finally, write

$$G(\rho) = \frac{\sqrt{\rho^2-1}}{\cosh^{-1}\rho} \qquad \text{(A-13)}$$

Substituting these results in eq A-9,

$$\left.\begin{aligned} \overline{H_\phi(x)} &= -\frac{\sec\beta_s\ell}{\eta_0(1-\nu^2)}\,G(\rho)\Big\{j[E_y^e(0)-\nu\eta_0H_z^e(0)]\sin[\beta_s(x-\ell)] \\ &\quad +[\nu E_y^e(0)-\eta_0H_z^e(0)][\exp(-j\beta_e x)\cos\beta_s\ell-\exp(-j\beta_e\ell)\cos\beta_s x]\Big\} \\ \overline{E_r(x)} &= \frac{\sec\beta_s\ell}{1-\nu^2}\,G(\rho)\Big\{[E_y^e(0)-\nu\eta_0H_z^e(0)]\cos[\beta_s(x-\ell)] \\ &\quad -[\nu E_y^e(0)-\eta_0H_z^e(0)][\nu\exp(-j\beta_e x)\cos\beta_s\ell+j\exp(-j\beta_e\ell)\sin\beta_s x]\Big\} \end{aligned}\right\} \qquad \text{(A-14)}$$

$0 \le x \le \ell;\ 0 \le \nu < 1$

which are eq 10 of the main text.

Appendix B

Short Circuit Terminations: Proof that $I_c^o \to I_c^i$ for $\ell \ll \lambda c$

From the second of eq 31, for small ℓ

$$\underline{V}_c^o \simeq (\underline{I} + j\underline{P}_c^i\beta_c\ell)\underline{S}_c^{-1}\underline{K}_c(\ell) + \underline{U}_c(\ell) \tag{B-1}$$

where, by eq 30,

$$\underline{S}_c \simeq (\underline{P}_c^i + \underline{P}_c^o) + j(\underline{I} + \underline{P}_c^o\underline{P}_c^i)\beta_c\ell$$

From eq 51

$$\underline{U}_c(\ell) \simeq \ell\underline{E}_c^e$$

$$\underline{ZW}_c(\ell) \simeq -j(\beta_c\ell^2/2)\underline{E}_c^e$$

Therefore,

$$\underline{K}_c(\ell) \simeq -j(\beta_c\ell^2/2)\underline{E}_c^e - \underline{P}_c^o\ell\underline{E}_c^e \simeq -\underline{P}_c^o\ell\underline{E}_c^e \tag{B-2}$$

Using eq 50

$$(\underline{I} + j\underline{P}_c^i\beta_c\ell) = (\underline{I} + jk^i\underline{P}\beta_c\ell) = \underline{T}\,, \tag{B-3}$$

say:

$$\underline{S}_c = (k^i + k^o)\underline{P} + j(\underline{I} + k^ok^i\underline{P}^2)\beta_c\ell$$

$$\underline{K}_c(\ell) = -k^o\underline{P}\ell\underline{E}_c^e$$

Then, we have

$$\begin{aligned}\underline{V}_c^o &\simeq [\underline{T}\underline{S}_c^{-1}(-k^o\underline{P}) + \underline{I}]\ell\underline{E}_c^e \\ &= (\underline{I} - k^o\underline{T}\underline{S}_c^{-1}\underline{P})\ell\underline{E}_c^e \\ &= \left[\frac{\underline{P}^{-1}}{k^o}\underline{S}_c\right] - \underline{T}\,\underline{S}_c^{-1}k^o\underline{P}\ell\underline{E}_c^e \end{aligned} \tag{B-4}$$

but

$$\begin{aligned}\frac{\underline{P}^{-1}}{k^o}\underline{S}_c - \underline{T} &= \frac{\underline{P}^{-1}}{k^o}[(k^i + k^o)\underline{P} + j(\underline{I} + k^ok^i\underline{P}^2)\beta_c\ell] - (\underline{I} + jk^i\underline{P}\beta_c\ell) \\ &= \frac{k^i}{k^o}\underline{I} + j\frac{\underline{P}^{-1}}{k^o}\beta_c\ell + \frac{k^i}{k^o}\underline{I}\end{aligned}$$

for $\ell \ll \lambda_c$.

Therefore,

$$V_c^o \to \frac{k^i}{k^o}(jk^ok^i\underline{P}^2)^{-1}\frac{1}{\beta_c\ell}k^o\underline{P}\ell\underline{E}_c^e = \frac{\underline{P}^{-1}\underline{E}_c^e}{jk^o\beta_c} \to 0 \text{ as } \underline{P} \to \infty \tag{B-5}$$

However,

$$\underline{I}_c^o = \underline{Y}_c^o\underline{V}_c^o = k^o\underline{Y}\underline{P}\frac{\underline{P}^{-1}\underline{E}_c^e}{jk^o\beta_c} = \frac{\underline{Y}\underline{E}_c^e}{j\beta_c} = \underline{I}_c^i \text{ ; Q.E.D.} \tag{B-6}$$

Appendix C

Derivation of Formula for Transfer Impedance for Class II and Class IV Definitions and Measurements

For Class II we have

$$\overline{H}_\phi = \text{constant} = -\frac{I_g}{2\pi a}$$

$$\overline{E}_r \equiv 0$$

and, therefore,

$$E_c^e = -\frac{j\omega I_g}{2\pi a} L_c^e$$

$$H_c^e \equiv 0$$

Furthermore,

$$P_c^i \to \infty \; ; \; P_c^o = 0$$

such that:

$$U_c = \frac{\sin \beta_c \ell}{\beta_c} E_c^e$$

$$K_c = -\frac{j(1 - \cos \beta_c \ell)}{\beta_c} E_c^e$$

$$S_c = P_c^i \cos \beta_c \ell + j(1 + P_c^o P_c^i)\sin \beta_c \ell$$

$$= P_c^i(\cos \beta_c \ell + jP_c^o \sin \beta_c \ell) + j\sin \beta_c \ell$$

$$= P_c^i \cos \beta_c \ell + j\sin \beta_c \ell$$

$$V_c^o = \frac{\cos \beta_c \ell + jP_c^i \sin \beta_c \ell}{P_c^i \cos \beta_c \ell + j\sin \beta_c \ell}\left(\frac{-j}{\beta_c}\right)(1 - \cos \beta_c \ell)E_c^e + \frac{\sin \beta_c \ell}{\beta} E_c^e$$

$$\to \frac{j\sin \beta_c \ell}{\cos \beta_c \ell}\left(\frac{-j}{\beta_c}\right)(1 - \cos \beta_c \ell)E_c^e + \frac{\sin \beta_c \ell}{\beta_c} E_c^e$$

and

$$V_c^o = \frac{\tan \beta_c \ell}{\beta_c}(1 - \cos \beta_c \ell)E_c^e + \frac{\sin \beta_c \ell}{\beta_c} E_c^e$$

For small ℓ, the last result becomes

$$V_c^o \simeq \frac{\beta_c \ell}{\beta_c}[(\beta_c^2 \ell^2/2)E_c^e + \frac{\beta_c \ell}{\beta_c} E_c^e$$

$$= \ell E_c^e[(\beta_c^2 \ell^2/2) + 1] \to \ell E_c^e = -\frac{j\omega I_g}{2\pi a} \ell L_c^e$$

and

$$Z_T = -\frac{V_c^o}{I_g \ell} = \frac{j\omega L_c^e}{2\pi a}$$

A formula for transfer impedance for Class IV definition follows by appropriate permutation of symbols.